



**HAL**  
open science

## **Oxidative stress response in pulmonary cells exposed to different fractions of PM<sub>2.5-0.3</sub> from urban, traffic and industrial sites**

Lamia Moufarrej, Anthony Verdin, Fabrice Cazier, Frédéric Ledoux,  
Dominique Courcot

### ► **To cite this version:**

Lamia Moufarrej, Anthony Verdin, Fabrice Cazier, Frédéric Ledoux, Dominique Courcot. Oxidative stress response in pulmonary cells exposed to different fractions of PM<sub>2.5-0.3</sub> from urban, traffic and industrial sites. *Environmental Research*, 2023, 216 (Part 2), pp.114572. 10.1016/j.envres.2022.114572 . hal-03821902

**HAL Id: hal-03821902**

**<https://ulco.hal.science/hal-03821902>**

Submitted on 20 Oct 2022

**HAL** is a multi-disciplinary open access archive for the deposit and dissemination of scientific research documents, whether they are published or not. The documents may come from teaching and research institutions in France or abroad, or from public or private research centers.

L'archive ouverte pluridisciplinaire **HAL**, est destinée au dépôt et à la diffusion de documents scientifiques de niveau recherche, publiés ou non, émanant des établissements d'enseignement et de recherche français ou étrangers, des laboratoires publics ou privés.

1 **Oxidative stress response in pulmonary cells exposed to different fractions of PM<sub>2.5-0.3</sub>**  
2 **from urban, traffic and industrial sites**

3  
4 Lamia MOUFARREJ<sup>1</sup>, Anthony VERDIN<sup>1</sup>, Fabrice CAZIER<sup>2</sup>, Frédéric LEDOUX<sup>1\*</sup>, and  
5 Dominique COURCOT<sup>1</sup>

6  
7 <sup>1</sup> Unité de Chimie Environnementale et Interactions sur le Vivant, UCEIV UR4492, SFR  
8 Condorcet FR CNRS 3417, Univ. Littoral Côte d'Opale, 145 avenue Maurice Schumann,  
9 59140 Dunkerque, France

10  
11 <sup>2</sup> Centre Commun de Mesures, Univ. Littoral Côte d'Opale, 145 avenue Maurice Schumann,  
12 59140 Dunkerque, France

13  
14 \*Corresponding author: frederic.ledoux@univ-littoral.fr  
15

16 **Abstract**

17           The aim of this work was to study the relationship between oxidative stress damages  
18 and particulate matter (PM) chemical composition, sources, and PM fractions. PM<sub>2.5-0.3</sub> (PM  
19 with equivalent aerodynamic diameter between 2.5 and 0.3 µm) were collected at urban, road  
20 traffic and industrial sites in the North of France, and were characterized for major and minor  
21 chemical species. Four different fractions (whole PM<sub>2.5-0.3</sub>, organic, water-soluble and non-  
22 extractable matter) were considered for each of the PM<sub>2.5-0.3</sub> samples from the three sites. After  
23 exposure of BEAS-2B cells to the four different fractions, oxidative stress was studied in cells  
24 by quantifying reactive oxygen species (ROS) accumulation, oxidative damage to proteins  
25 (carbonylated proteins), membrane alteration (8-isoprostane) and DNA damages (8-OHdG).  
26 Whole PM<sub>2.5-0.3</sub> was capable of inducing ROS overproduction and caused damage to proteins  
27 at higher levels than other fractions. Stronger cell membrane and DNA damages were found  
28 associated with PM and organic fractions from the urban site. ROS overproduction was  
29 correlated with level of expression of carbonylated proteins, DNA damages and membrane  
30 alteration markers. The PM<sub>2.5-0.3</sub> collected under industrial influence appears to be the less  
31 linked to cell damages and ROS production in comparison with the other influences.

32

33 **Keywords:** Particulate matter; oxidative stress; reactive oxygen species; 8-isoprostane; 8-  
34 OHdG; carbonylated proteins.

## 35 1. Introduction

36 Numerous studies have been conducted to study chemical atmospheric particulate matter (PM)  
37 characteristics (Telesiński and Kiepas-Kokot, 2021), and to better understand the impact of PM  
38 on human health (Broome et al., 2020; Fischer et al., 2020; Guan et al., 2021; Lin et al., 2020;  
39 P. Wang et al., 2021; Zhang et al., 2021). Results have shown associations between PM and  
40 cardiovascular disease (Aryal et al., 2021), fertility (L. Wang et al., 2021), cancer (Gogna et al.,  
41 2019; Nagel et al., 2018), increased risk of autism spectrum disorders (Lam et al., 2016),  
42 psychiatric disorders (Buoli et al., 2018; Chen et al., 2018; Oudin et al., 2016). PM has been  
43 proven to cause damaging respiratory outcomes, especially through the triggering of oxidative  
44 stress (Li et al., 2021; Mu et al., 2021; Quezada-Maldonado et al., 2021) which is one of the  
45 first mechanism of stress appearing in the cell. Oxidative stress occurs in the cell when a break  
46 in the redox homeostasis happens, due to a decrease in antioxidant capacity, or an  
47 overproduction of reactive oxygen species (ROS) such as superoxide anion ( $O_2^{\cdot-}$ ), hydrogen  
48 peroxide ( $H_2O_2$ ), hydroxyl radical ( $OH\cdot$ ). This phenomenon may lead to non-specific and  
49 irreversible oxidation of DNA, proteins and cellular lipids (Badran et al., 2020a; Migdal and  
50 Serres, 2011; Ndong Ba et al., 2019). Along with the direct measurement of ROS in the cells,  
51 different cellular methods could be used for oxidative stress evaluation. Among the biomarkers  
52 used for oxidative stress assessment (Ho et al., 2013): 8-hydroxy-2'-deoxyguanosine (8-OHdG)  
53 is one of the predominant forms of ROS-induced oxidative DNA damage, isoprostanes are  
54 generated by the peroxidation of a polyunsaturated fatty acid (Morrow et al., 1992), and  
55 carbonylated proteins, are an indicator of oxidative alteration of proteins. The PM induced  
56 oxidative stress has been linked to metals (Jan et al., 2020) and organic compounds (Badran et  
57 al., 2020a, Win et al., 2018). In addition, the ability of the particles themselves (Dergham et al.,  
58 2015, 2012; Leclercq et al., 2018; Moufarrej, 2021), their organic extract (OE) (Abbas et al.,  
59 2019; Badran et al., 2020b; Billet et al., 2018) or their water soluble extract (WSE) (X. Liu et

60 al., 2020; Shuster-Meiseles et al., 2016; Xu et al., 2018; Yan et al., 2017) to induce oxidative  
61 stress has been shown. Despite the numerous studies investigating the relationship between PM  
62 physical-chemical properties and oxidative stress, a lack of information remains regarding the  
63 fraction of PM that contributes the most in triggering of oxidative stress. This study aims to  
64 investigate the dependence of oxidative stress to PM chemical composition, sources, and PM  
65 fractions. In this work, different PM samples were collected under urban, industrial, and road  
66 traffic influence in northern France, as the whole population is mainly exposed to such kind of  
67 emission sources. The ROS, 8-isoprostane, carbonylated proteins and 8-OHdG were quantified  
68 to assess the onset of oxidative stress. Correlations, principal component analysis, and  
69 classifications were used to reveal the relationship between oxidative stress, different PM  
70 fractions, and PM chemical composition.

71

## 72 2. **Material and methods**

### 73 2.1. PM sampling sites

74 PM with an equivalent aerodynamic diameter between 2.5 and 0.3  $\mu\text{m}$  ( $\text{PM}_{2.5-0.3}$ ) were collected  
75 in different sites in northern France. Five samples were collected under urban influence, in  
76 Dunkirk (51°01'35.8"N 2°22'20.0"E): one annual average sample (U-Y) March 19, 2014 to  
77 March 18, 2015, and four seasonal samples: U-Sp during spring period (March 19, 2014 to June  
78 21, 2014), U-Su during summer period (June 21 to September 26, 2014), U-A during autumn  
79 period (September 27 to December 17, 2014) and U-W during winter period (December 18,  
80 2014 to March 18, 2015). In addition to these five samples, one sample (I) was collected under  
81 industrial influence at Grande-Synthe (51°01'29.0"N 2°18'11.7"E), near integrated steelworks  
82 and chemical activities (steam cracking, oil stocks) between February 28, 2017 and June 02,  
83 2017. Finally, another sample (T) was collected in a road traffic influenced site at Roubaix  
84 (50°42'24.6"N 3°10'49.8"E) between March 02, 2017 and June 1, 2017. All these seven samples

85 were collected using 5 stages plus back up cascade impactor (Staplex<sup>®</sup> 235, TFIA, 68 m<sup>3</sup>/h) and  
86 PM<sub>2.5-0.3</sub> were retrieved from the 5 impaction plates (cut-off off the 5<sup>th</sup> plate was 0.33 μm) as  
87 described elsewhere (Borgie et al. 2015).

88

## 89 2.2. Preparation of the different PM fractions

90 PM samples were studied by considering them as whole PM, water-soluble extract (WSE),  
91 organic extract (OE) and non-extractable matter (dPM). In order to prepare the WSE for each  
92 sample, 60 mg of PM<sub>2.5-0.3</sub> were extracted with 3 mL of ultra-pure water in a glass conical tube,  
93 using ultrasonic treatment for 20 minutes, and then centrifuged for 10 minutes at 4°C and 2500  
94 g. The supernatant was then transferred in a polyethylene vial, and the particle pellet was again  
95 suspended in ultrapure water, and the recovery steps were repeated twice (Landkocz et al.,  
96 2017). Finally, the WSE was filtered through a nylon filter (0.22 μm) (and stored at -18 °C until  
97 use. The same steps were followed to prepare the OE, using dichloromethane as a solvent.  
98 Finally, the obtained extract was concentrated under nitrogen flow, and dimethyl sulfoxide was  
99 added to the residue for solvent change. Finally, in order to prepare the dPM, the particulate  
100 residue after successive extraction of both organic and water-soluble fractions was considered.

101

## 102 2.3. PM chemical characterization

103 PM<sub>2.5-0.3</sub> were extensively characterized. Briefly, major and trace elements were quantified in  
104 whole PM samples as well in WSE using Inductively Coupled Plasma coupled to Atomic  
105 Emission Spectrometry or Mass spectrometry (ICP-AES and ICP-MS). Major water-soluble  
106 ions were quantified after water leaching using ion chromatography. Total Carbon was  
107 quantified using C, H, N, S microanalyzer. Polycyclic Aromatic Hydrocarbons (PAHs) were  
108 quantified in the OE after Soxhlet extraction of PM<sub>2.5-0.3</sub> using dichloromethane. Detailed  
109 procedures used for chemical characterization can be found in Landkocz et al, 2017.

110

#### 111 2.4. Cell culture

112 BEAS-2B cells are used in this work. They were initially generated from normal human  
113 bronchial epithelial cells from non-cancerous subjects. BEAS-2B (ATCC® CRL-9609™,  
114 ECACC, Wiltshire, UK) were cultured in Corning cellbind® plastic plates or flasks  
115 (ThermoFisher, France) using LHC9 (ThermoFisher, France) as culture medium and incubated  
116 at 37°C in a humidified atmosphere containing 5% CO<sub>2</sub>. Medium was replaced every three days  
117 and cells were passed when reaching 80% of confluence.

118

#### 119 2.5. Cytotoxicity

120 The WST-1 assay allows the evaluation of mitochondrial activity and cell proliferation. WST-1  
121 cytotoxicity test was performed in order to choose the dose of exposure allowing the  
122 observation of a cellular response without massive cell mortality. The WST-1 colorimetric  
123 assay kit was purchased from Roche Diagnostics GmbH (Mannheim, Germany). In the present  
124 study, we would like to expose to a unique dose to be able to discriminate the 28 samples (7  
125 sites and 4 different fractions). The heterogeneity of the 28 samples makes this dose more  
126 difficult to define. Cells were exposed to PM, WSE, OE and dPM fractions of the different  
127 samples using different doses (6, 12, 24, 48 and 96 µg/cm<sup>2</sup>), using four replicates for each  
128 sample, and during 48 h. Exposure of BEAS-2B cells to the different PM<sub>2.5-0.3</sub> samples showed  
129 strong significant decrease in mitochondrial activity after 48 h of exposure, at 48 and 96 µg/cm<sup>2</sup>.  
130 For low doses (6 and 12 µg/cm<sup>2</sup>), very weak responses were recorded. For the 24 µg/m<sup>3</sup> dose,  
131 the samples showed medium decreases in mitochondrial activity. Considering all conditions of  
132 exposure, the 24 µg/cm<sup>2</sup> dose appeared to be the most suitable dose for studying the oxidative  
133 stress parameters, providing sufficient doses to cause certain adverse effects, without massive

134 cell death, and for comparing responses associated with the four fractions of the seven PM<sub>2.5-</sub>  
135 <sub>0.3</sub> samples. It was therefore chosen as the exposure dose for the whole study.

136

## 137 2.6. Inflammation

138 The protein expression of the inflammatory cytokine IL-6 was quantified after 48 h of cell  
139 exposure to the different PM fractions. The test was done using ELISA sandwich method, using  
140 Human IL-6 kit (ELISA MAX™ Deluxe Set, BioLegend, San Diego, CA, USA) according to  
141 manufacturer's protocol.

142

## 143 2.7. Oxidative stress

144 Oxidative stress was evaluated by the measurement of ROS overproduction, lipid membrane  
145 alteration, and the measurement of protein and DNA damage.

146

### 147 ROS assay

148 Cells were cultivated in 96 well black plates according to the manufacturer's instructions. This  
149 test was performed 48 h after the exposure (40,000 cells/well) using the DHE  
150 (Dihydroethidium) Assay Kit—Reactive Ox Species (ab236206, Abcam China, Shanghai,  
151 China), according to manufacturer's protocol. It allows the quantification of reactive oxygen  
152 Species (Superoxide radical and hydrogen peroxide) in living cells, and uses dihydroethidium  
153 DHE as a fluorescent probe for the detection of ROS.

154

### 155 *Assessment of oxidative DNA damage - quantification of 8-OHdG*

156 8-hydroxy-2'-deoxyguanosine (8-OHdG) is formed as a result of oxidative damage to DNA by  
157 reactive oxygen and nitrogen species. The concentration of 8-OHdG was measured using  
158 8-hydroxy-2'-deoxyguanosine ELISA Kit, (ab201734, Cayman, Ann Arbor, MI, USA),

159 according to manufacturer's protocol. The assay uses a plate coated with 8-hydroxy-2'-  
160 deoxyguanosine, and an antibody, bound to the enzyme horseradish peroxidase (HRP) for  
161 detection (Ndong Ba et al., 2019).

162

### 163 *Assessment of oxidative lipid damage - quantification of 8-isoprostane*

164 Isoprostanes are a family of eicosanoids of non-enzymatic origin, produced by the oxidation of  
165 the phospholipids tissue by ROS. The 8-isoprostane competitive ELISA assay (Abcam  
166 ab175819<sup>®</sup>, Cambridge, UK) was used for the determination of 8-isoprostanes in cells,  
167 according to manufacturer's protocol.

168

### 169 *Assessment of protein oxidative damage - quantification of carbonylated proteins*

170 Protein carbonylation is one of the irreversible oxidative modifications of proteins. The method  
171 based on the reaction of 2,4-Dinitrophenylhydrazine (DNPH) with carbonylated proteins. The  
172 DNP-hydrazone formed can be quantified by measuring its absorbance at 375 nm. Levels of  
173 carbonyl groups were determined using Protein Carbonyl Content Assay kit (Abcam  
174 ab126287<sup>®</sup>, Cambridge, UK) according to manufacturer's protocol (Ndong Ba et al., 2019).

175

## 176 2.8. Statistical analysis

177 Toxicity test results are normalized to the control, and are presented as an average of the 4  
178 replicates for cytotoxicity and inflammation tests, and as an average of the 3 replicates for  
179 oxidative stress tests, considering the standard deviation. The nonparametric Mann-Whitney U  
180 test was performed to compare the values obtained with the controls. Significant differences  
181 are reported with values of  $p < 0.05$  (\*),  $p < 0.01$ (\*\*) and  $p < 0.001$  (\*\*\*)).

182 Correlations were studied using the Spearman coefficient as the normality of the distribution  
183 was not verified (Shapiro-Wilk test,  $p < 0.001$ ) for most of the variables. Two levels of

184 significance were considered,  $p < 0.05$  and  $p < 0.001$ , allowing conclusions about correlation  
185 with 95% and 99.9% confidence, respectively. In addition, the data were also examined using  
186 the Principal Component Analysis (PCA), which was performed considering  $n=84$  samples  
187 including triplicates (7 PM samples x 4 fractions x 3 replicates).

188

### 189 3. Results

#### 190 3.1. PM<sub>2.5-0.3</sub> chemical composition

191 First of all, in relation with the procedure required to prepare samples for chemical analysis and  
192 to prepare the four fractions of PM<sub>2.5-0.3</sub>, it can be noticed that the ion composition was the same  
193 in the WSE and the whole PM<sub>2.5-0.3</sub>. As well, the PAHs composition was similar for the PM<sub>2.5-</sub>  
194 <sub>0.3</sub> fraction and OE. No water-soluble and no PAH compound have been detected in the dPM  
195 samples.

196 Table 1 gathers the average composition of the 7 PM<sub>2.5-0.3</sub> samples. Total carbon (11.3 - 19.0%),  
197 NO<sub>3</sub><sup>-</sup> (8.1 - 14.3%), SO<sub>4</sub><sup>2-</sup> (4.0 - 8.3%), Cl<sup>-</sup> (0.4 - 8.6%), Ca<sup>2+</sup> (3.7 - 5.8%), Na<sup>+</sup> (0, 4 - 5.0 %),  
198 NH<sub>4</sub><sup>+</sup> (1.3 - 2.3 %), Fe (3.1 - 8.7 %) and Al (1.2 - 3.4 %) represented major compounds of the  
199 particles. In the "Urban" samples (U-PM), these species explained between 52.6% (summer)  
200 and 58.3% (winter) of the PM mass, compared to 51.7% in the "Traffic" PM (T-PM) and 57.5%  
201 in the "Industrial" one (I-PM). Considering the urban site, NO<sub>3</sub><sup>-</sup> ions were detected in higher  
202 amount in spring than in other seasons, partly due to meteorological conditions favoring their  
203 accumulation in the atmosphere (Favez et al., 2012;). NO<sub>3</sub><sup>-</sup> ions were already shown to be the  
204 preponderant species of secondary inorganic ions in the Region (Kfoury et al. 2016, Ledoux et  
205 al. 2017). The highest proportion of NO<sub>3</sub><sup>-</sup> is observed in the T-PM sample (14.3%), and this  
206 could be related to the high concentration of NO<sub>x</sub> observed at this site (Atmo Hauts-de-France  
207 air quality network), which are well known to be converted in the atmosphere into nitrate  
208 species (Seinfeld and Pandis, 2006). Na<sup>+</sup> and Cl<sup>-</sup> ions are known to be associated with marine

209 aerosols, whose contribution may be significant at the study area due to the proximity with the  
210 English Channel-North Sea area. At the urban site, higher C content was detected in particles  
211 sampled in autumn and winter. This could be explained by colder temperatures during these  
212 seasons and therefore, a higher contribution of emissions related to residential heating using  
213 fossil fuels. The metal element contents Al (1.2 - 3.4%) and Fe (3.1 - 8.7%) can be explained  
214 by crustal and anthropogenic emissions, with however a significant contribution of industrial  
215 emissions in samples collected at the industrial site (Kfoury et al., 2016). In particular, it should  
216 be noticed that Fe and Mn contents were respectively 2.3 and 3.8 times higher in the I-PM  
217 sample, compared to the U-PM urban samples. Fe, Mn, Zn, Pb, Cr, and Cd could be linked to  
218 anthropogenic sources, especially to emissions from steelmaking and metallurgical activities  
219 (Kfoury et al., 2016). Cu, Zn and Cr contents clearly reflect the influence of traffic emissions  
220 (Gietl et al. 2010). In particular, the copper content at the T-PM site is 1.5 times higher than at  
221 the urban site (U-Y-PM), and more than 3 times higher than at the I-PM site. Table S1 gathers  
222 the chemical composition of the PM<sub>2.5-0.3</sub> WSE. Among the considered metals, Mn appeared as  
223 the most abundant element in the water-soluble fraction, far ahead of Sr and Ba, then Al, Cu,  
224 Zn, Mo and Ni. Fe was only detected in the WSE of PM<sub>2.5-0.3</sub> collected on the traffic and  
225 industrial site (Table S1). Among the 16 priority PAHs listed by the United States  
226 Environmental Protection Agency (USEPA), contents of dibenz[a,h]anthracene (5.9 - 11.6  
227 µg/g), indeno[1,2,3-c,d]pyrene (3.2 - 12.2 µg/g), chrysene (2.2 - 13.2 µg/g),  
228 benzo[b]fluoranthene (1.9 - 11.8 µg/g), benzo[g,h,i]perylene (2.1 - 9.6 µg/g) and  
229 benzo[a]pyrene (2.0 - 9.4 µg/g) in PM were predominant. The other compounds (fluoranthene,  
230 pyrene, benz[a]anthracene and benzo[k]fluoranthene) showed content levels below 5 µg/g,  
231 while the 6 PAHs composed of 2 and 3 rings showed contents below 1 µg/g. For the urban site,  
232 PAH contents were 3 to 4 times higher in autumn and winter than in spring and summer.  
233 Between these two periods, the PAH profile (Figure S1) differed mainly by the content of

234 chrysene (contribution of wood combustion and coal distillation (Telesiński and Kiepas-Kokot,  
 235 2021)) and benzo[b]fluoranthene (diesel vehicle emissions (Xing et al., 2022)). In parallel, the  
 236 higher PAH contents were found for the industrial sample with a total content of 136.4 µg/g,  
 237 which corresponds to a value between 2 and 8 times higher than that of the other sites. This  
 238 observation was in agreement with other studies conducted in this urban site impacted by  
 239 industrial emissions (Crenn et al., 2017; Landkocz et al., 2017). On the contrary, PAH contents  
 240 were lower at the road-traffic site (17.8 µg/g).

241

242 Table 1: Chemical composition (µg/g) of PM<sub>2.5-0.3</sub> particles collected under urban influence –  
 243 seasonal and yearly average (U-Sp, U-Su, U-A, U-W, U-Y), industrial influence (I), and traffic  
 244 influence (T).

245

	U-Sp	U-Su	U-A	U-W	U-Y	T	I
<b>Al</b>	21810	27136	31719	34171	28026	11869	23800
<b>As</b>	12.2	12.1	17.3	16.1	13.9	10.0	10.0
<b>Ba</b>	272	343	399	339	331	932	285
<b>Cd</b>	6.8	6.2	5.6	6.2	6.3	10.0	10.0
<b>Co</b>	10.3	7.9	7.4	7.0	8.7	13.4	19.8
<b>Cr</b>	136	136	181	152	144	251	266
<b>Cu</b>	583	538	803	691	639	933	276
<b>Fe</b>	41179	40666	31331	43747	37530	38078	87549
<b>Mn</b>	1880	1984	1235	1922	1767	555	6692
<b>Mo</b>	24.0	30.5	40.2	30.7	30.3	35.9	22.3
<b>Ni</b>	137	111	105	95.9	116	59.5	467
<b>P</b>	1303	1882	1509	783	1345	979	1030
<b>Pb</b>	226	179	263	271	234	210	246
<b>Sn</b>	56.5	61.5	116	128	78.3	270	46.8
<b>Sr</b>	149	116	98.2	120	126	153.5	140.9
<b>Ti</b>	474	370	269	316	369	1631	1288
<b>V</b>	122	110	76	118	108	72.8	134
<b>Zn</b>	1259	1117	1335	1440	1293	1257	1841
<b>Ca<sup>2+</sup></b>	52900	46200	34600	37800	44600	39667	37106
<b>K<sup>+</sup></b>	4300	4500	4900	4700	4500	8053	6677
<b>Mg<sup>2+</sup></b>	6800	6200	5200	6900	6500	2701	9307
<b>Na<sup>+</sup></b>	49700	39600	29300	50100	43300	30620	41178

<b>NH<sub>4</sub><sup>+</sup></b>	16800	15000	22900	21700	16400	14944	12497
<b>Cl<sup>-</sup></b>	63200	45300	51000	86700	60900	38855	54882
<b>NO<sub>3</sub><sup>-</sup></b>	126100	92900	80900	89900	100400	142872	116133
<b>SO<sub>4</sub><sup>2-</sup></b>	70600	83400	72100	76600	75200	40013	53062
<b>TC</b>	113300	135700	190200	142500	142500	160000	149000
<b>Naphthalene</b>	0.2	0.3	0.4	0.4	0.2	0.2	1.1
<b>Acenaphthylene</b>	0.1	0.1	0.3	0.3	0.1	0.1	0.2
<b>Acenaphthene</b>	0.0	0.0	0.0	0.0	0.0	0.0	0.0
<b>Fluorene</b>	0.1	0.1	0.3	0.3	0.2	0.1	0.3
<b>Phenanthrene</b>	0.7	0.8	1.8	1.8	1.0	0.5	1.9
<b>Anthracene</b>	0.1	0.2	0.3	0.4	0.3	0.2	0.6
<b>Fluoranthene</b>	1.1	0.9	4.1	4.4	2.1	0.9	6.0
<b>Pyrene</b>	0.8	0.8	3.7	3.8	1.8	0.8	5.2
<b>Benz[a]anthracene</b>	0.6	0.4	0.4	5.5	1.9	0.7	10.1
<b>Chrysene</b>	2.2	2.2	11.7	13.2	5.4	2.6	20.5
<b>Benzo[b]fluoranthene</b>	2.8	1.9	11.0	11.8	5.3	2.3	20.0
<b>Benzo[k]fluoranthene</b>	0.7	0.5	3.2	3.5	1.7	0.6	7.1
<b>Benzo[a]pyrene</b>	2.6	2.0	9.0	9.4	3.9	1.7	15.5
<b>Indeno[1,2,3-c,d]pyrene</b>	3.9	3.3	12.2	10.2	6.1	4.2	16.9
<b>Dibenz[a,h]anthracene</b>	6.7	5.9	11.3	11.6	8.9	2.6	18.2
<b>Benzo[g,h,i]perylene</b>	2.6	2.1	9.6	8.6	4.4	3.0	12.8
<b>TPAH</b>	25.1	21.5	79.3	85.1	43.2	17.8	136.4

246

247

### 248 3.2. Inflammation

249 PM and dPM fractions were shown to induce an increase in IL-6 secretion, significantly higher  
 250 than the OE fraction, while the WSE fraction seemed to have no effect (Figure S2). Indeed, a  
 251 significant increase in IL-6 concentration was observed for all PM and dPM samples (Table  
 252 S2). Concerning the organic extracts (OE), 5 samples caused significant increases in IL-6  
 253 secretion while no effect was observed with the water-soluble extracts (WSE). These results  
 254 are in line with numerous works that have previously demonstrated the development of an  
 255 inflammatory response after exposure of lung cells to whole PM samples collected under  
 256 different influences and in different locations (Cachon et al., 2014; Dieme et al., 2012; Dong et  
 257 al., 2019; Xu et al., 2018).

258

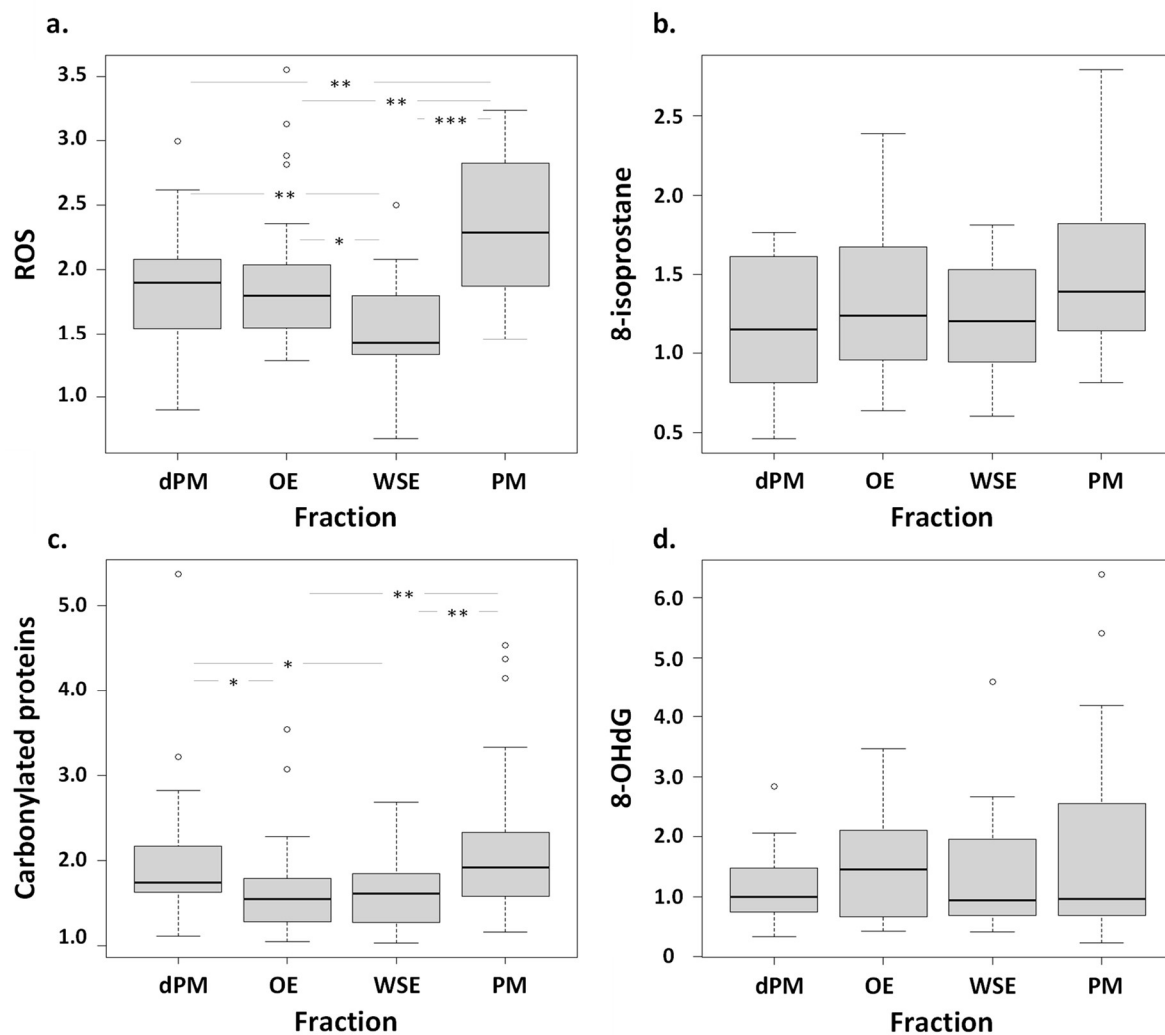
259 3.3. Oxidative stress

260 3.3.1. Reactive oxygen species

261 Regardless the site typology, considering the average response associated to the 4 fractions,  
262 PM<sub>2.5-0.3</sub> have significantly induced ROS accumulation in cells at higher levels than the other  
263 fractions (Figure 1-a). Looking into details, ROS production significantly increased ( $p < 0.05$ )  
264 following BEAS-2B exposure to all fractions of the PM<sub>2.5-0.3</sub> samples, except for some water-  
265 soluble extracts (U-A, U-Y and U-Sp) (Figure 2-a). The ROS overproduction was more  
266 pronounced for PM collected under urban and road traffic influences, and for the organic  
267 fraction of urban samples corresponding to cold seasons that appeared to be more concentrated  
268 in PAH (79 and 85  $\mu\text{g/g}$  PM for U-A-OE and U-W-OE respectively).

269

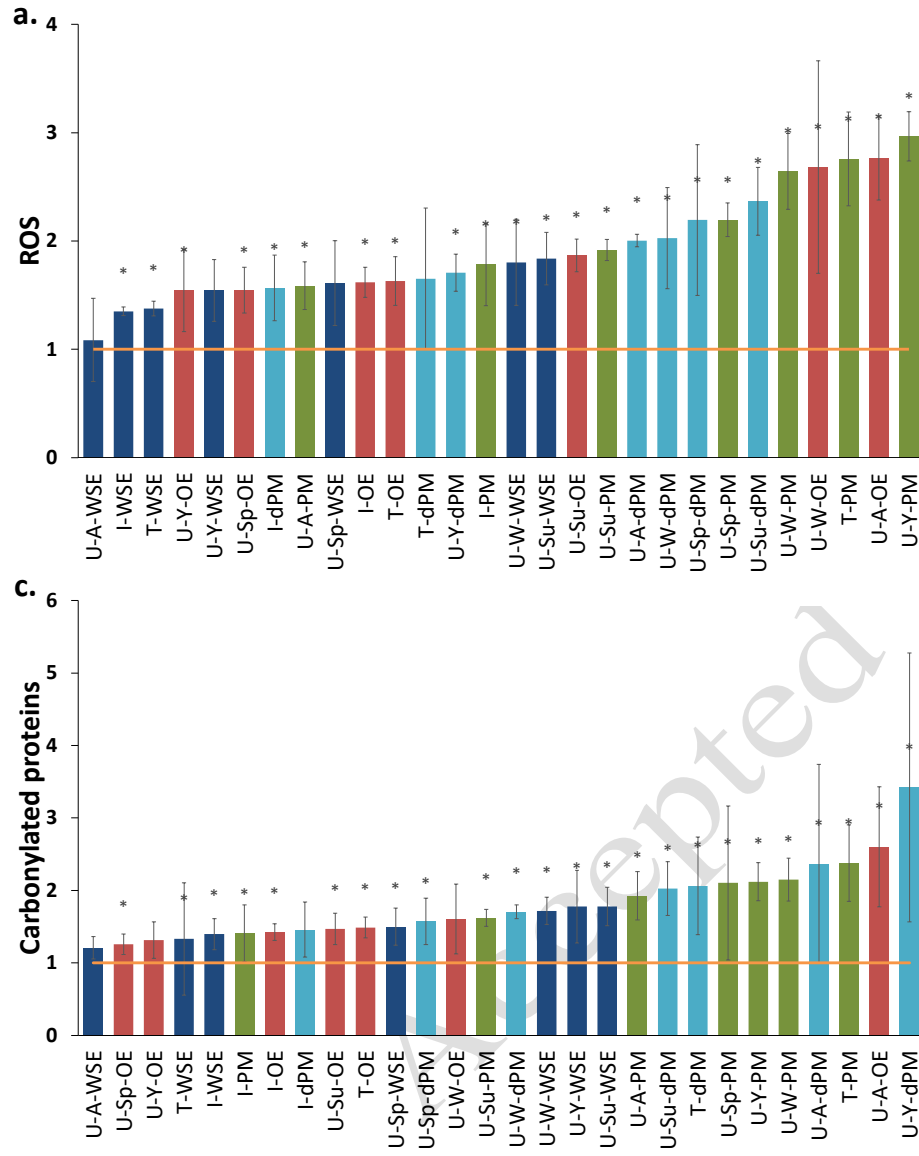
Accepted Manuscript



270

271 Figure 1: Concentration of (a) ROS, (b) 8-isoprostane, (c) carbonylated proteins and (d) 8-  
 272 OHdG, reported to total protein and control in BEAS-2B cells exposed to different fractions of  
 273 PM (dPM, OE, WSE, PM) at 24 µg/cm<sup>2</sup>. Results are represented by median and interquartile  
 274 ranges (n=21). Mann-Whitney test: \**p* <0.05; \*\**p* <0.01; \*\*\**p* <0.001.

275



277 Figure 2: Relative concentration of (a) ROS, (b) 8-isoprostane, (c) carbonylated proteins and  
278 (d) 8-OHdG, reported to total protein and control in BEAS-2B cells exposed to different  
279 fractions of PM collected under urban influence—seasonal and yearly average (U-Sp, U-Su, U-  
280 -A, U-W, U-Y), industrial influence (I), and traffic influence (T), at the dose 24  $\mu\text{g}/\text{cm}^2$ ,  
281 represented by means and standard deviations over three biological replicates. Mann-Whitney  
282 U-test vs. controls; \* $p < 0.05$  (Color code: green =PM; red=OE; light blue=dPM, dark  
283 blue=WSE).

284

### 285 3.3.2. 8-isoprostane

286 Whatever the fraction considered, there was no significant difference in the 8-isoprostane  
287 response after cell exposure (Figure 1-b). It is to note that U-Y was the sample inducing higher  
288 concentration of 8-isoprostane, followed by T-PM sample and its water-soluble extract (T-  
289 WSE). Whole  $\text{PM}_{2.5-0.3}$  appeared to be the fraction that is the most involved in the increase in  
290 8-isoprostane. The industrial sample (I-PM) did not appear to have any effect on the 8-  
291 isoprostane generation (Figure 2-b).

292

### 293 3.3.3. Carbonylated Proteins

294 PM and dPM fractions induced once again the stronger oxidative damages compared to OE and  
295 WSE (Figure 1-c). The concentration of carbonylated proteins significantly increased ( $p < 0.05$ )  
296 after exposure of BEAS-2B cells to the majority of the PM fractions. Indeed, only 4 samples  
297 (U-A-WSE, U-Y-OE, I-dPM and U-W-OE) did not induce a significant increase of  
298 carbonylated proteins concentration (Figure 2-c).

299

### 300 3.3.4. 8-OHdG

301 In average, there was no significant difference between the 8-OHdG concentration after cell  
 302 exposure to the different fractions (Figure 1-d). However, the PM fractions and OE would  
 303 appear to be the more involved in DNA damages: U-A-PM, U-Sp-PM and U-A-OE, U-W-OE,  
 304 and U-Sp-OE caused a significant increase in 8-OHdG formation (Figure 2-d). The samples  
 305 collected under the influence of road traffic and industrial emissions did not exhibit any  
 306 response whatever the fraction considered, and the same observation was made for the urban  
 307 samples collected in spring and summer.

308

### 309 3.4. Correlation analysis

310 The ROS concentrations showed weak correlations with the concentration data of 8-OHdG  
 311 ( $r=0.28$ ), 8-isoprostane ( $r=0.26$ ), and IL-6 ( $r=0.33$ ) (Table 2). On the other hand, ROS  
 312 concentrations were strongly correlated with carbonylated protein concentrations ( $r=0.67$ ).  
 313 Carbonylated proteins also showed weak correlations with IL-6 ( $r=0.29$ ) and moderate  
 314 correlations with 8-isoprostane ( $r=0.44$ ). Concerning correlation with the chemical composition  
 315 (Table S3), positive correlations were found between ROS accumulation and several elements  
 316 (Cd:  $r=0.43$ ,  $p < 0.05$ ; Sr:  $r=0.55$ ,  $p < 0.01$ ), protein oxidation (Al:  $r=0.42$ ,  $p < 0.05$ ; As:  $r=$   
 317  $0.50$ ,  $p < 0.05$ ; Cu:  $r=0.45$ ,  $p < 0.05$ ; Pb:  $r=0.43$ ,  $p < 0.05$ ). Positive correlations were also  
 318 evidenced between cell membrane alteration and some elements (Al:  $r=0.54$ ,  $p < 0.01$ ; As:  
 319  $r=0.48$ ,  $p < 0.05$ ).

320

321 Table 2: Correlation coefficient (Spearman) between cell parameters (n=96). Only correlations  
 322 with  $p < 0.05$  are reported (\*\* $p < 0.01$ ; \*\*\*  $p < 0.001$ ).

	IL-6	ROS	Carbonylated proteins	8-OHdG	8-isoprostane
IL-6		0.33**	0.29**		
ROS	0.33**		0.67***	0.28**	0.26

<b>Carbonylated proteins</b>	0.29**	0.67***	0.30**	0.44***
<b>8-OHdG</b>		0.28**	0.30**	
<b>8-isoprostane</b>		0.26	0.44***	

323

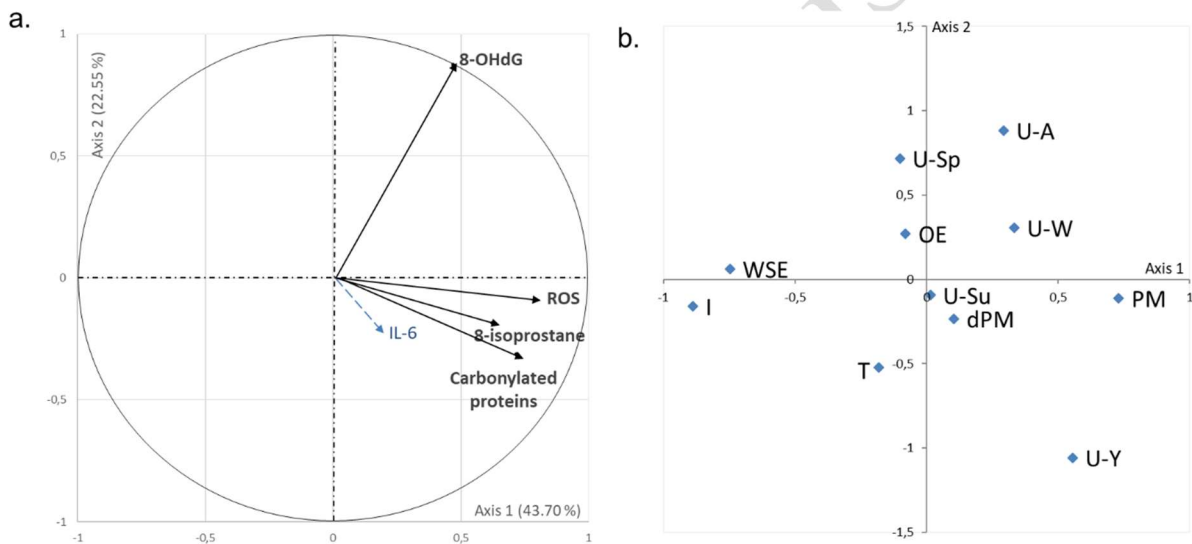
### 324 3.5. Principal component analysis

325 PCA was performed considering 84 samples including triplicates. The first axis explained about  
326 44% of the variability of the data, and appeared to be strongly related to the amount of ROS, 8-  
327 isoprostane and carbonylated proteins (Figure 3-a). Thus, this axis is clearly related to the  
328 capacity of the samples to induce damage to the cell membrane and proteins. Axis 2 explained  
329 about 22% of the variability of the data, and appeared to be related to DNA damages. Note that  
330 the 8-OHdG variable appeared to be totally uncorrelated with the other oxidative stress  
331 parameters. Similarly, IL6 considered as supplementary variable, showed poor relationship  
332 with the oxidative damage parameters in this plan (1,2) explaining 66% of the variability in the  
333 data. The 84 samples were categorized according to their influence and the fractions they belong  
334 to. The barycenters relative to the 4 fractions of the same influence (T, I, U-Sp U-Su, U-A U-  
335 W and U-Y) and those relative to all the influences of the same fraction (PM, dPM, OE and  
336 WSE) were projected in the (1,2) plane (Figure 3-b) in order to highlight links between the  
337 latter and the 4 oxidative stress parameters. The axis 1 which is associated to damage to the  
338 membrane and proteins and ROS overproduction, shows a ranking WSE < OE and dPM < PM  
339 evidencing the capacity of the latter to induce the more cell damages and WSE to induce less  
340 cell damages. It appears in agreement with the previous observations made on each of the  
341 parameters (Figures 1 and 2).

342 If we adopt the same reasoning, focusing now on the influences, it appears that the industrial  
343 influence appears to be the less linked to cell damages and ROS production in comparison with  
344 the other influences.

345 Another interesting observation can be made. In this work, we considered 4 seasonal samples  
346 and an average annual sample (made up of 25% of each seasonal sample) for the Urban site. It  
347 appears that the projection of the characteristics of this average sample (U-Y) is not in the center  
348 of those of the seasonal samples. This illustrates that the response of cells exposed to particles  
349 from the annual sample is not an average of the ones observed after cell exposure to particles  
350 from seasonal samples. This tends to show and prove that complex interactions could take place  
351 between the compounds of these samples, and that these interactions would be able to modulate  
352 the cell responses to oxidative stress, and the resulting damages.

353



354

355

356 Figure 3: (a) PCA performed considering the 4 parameters ROS, 8-OHdG, carbonylated  
357 proteins, and 8-isoprostane, on n=84 samples - (b) Representation of the barycenters of the  
358 different fractions or influences in the (1,2) plane.

359

360 To go further, a hierarchical classification on the principal components was performed in order  
361 to statistically evidence group samples and highlight their specificity (depending on sampling  
362 sites, fractions and cellular parameters) (Table 3). Three groups are highlighted (the

363 associations mentioned below are statistically significant at  $p < 0.05$ ): The first group ( $n=28$ ) is  
364 mostly related to the industrial influence ( $p < 0.01$ ) and to the water-soluble fractions of the  
365 different PM samples. It is characterized by low values for ROS, carbonylated proteins and 8-  
366 isoprostane parameters ( $p < 0.001$  for these three parameters). With a lower statistical weight,  
367 low values of parameters 8-OHdG ( $p=0.06$ ) and IL-6 ( $p=0.1$ ) seem to be associated with this  
368 group. The second group ( $n=45$ ) is characterized, by high values of ROS ( $p < 0.01$ ) and 8-  
369 isoprostane ( $p < 0.01$ ) and low values for 8-OHdG. This class is strongly represented by the  
370 urban influence, especially U-Su ( $p < 0.01$ ). The industrial influence do not statistically belong  
371 to this group ( $p < 0.05$ ). The third and last group ( $n=11$ ) is characterized by high ROS values ( $p$   
372  $< 0.001$ ) and damage parameters (8-isoprostane and especially 8-OHdG ( $p < 0.001$ )). The  
373 samples associated with this third group are responsible for more damages compared to the  
374 other samples and cause a more marked disruption of cell function. In particular, the U-A  
375 influence stands out. The WSE fraction is statistically less associated with this 3rd group ( $p$   
376  $< 0.05$ ) showing that WSE is not the most involved fraction of  $PM_{2.5-0.3}$  in ROS overproduction.  
377 The test value for the PM fraction also seems to show that this 3rd group would be related to  
378 the PM fraction ( $p = 0.13$ ). The study of the barycentres of the fractions (Figure 3-b) tends to  
379 support this hypothesis.

380

381 Table 3: Test values obtained for the "Fraction" and "Influence" categories and for the  
382 quantitative variables associated to each of the classes identified after Principal Component  
383 Analysis followed by Hierarchical Cluster Analysis. The test value allows to highlight the  
384 characteristics that differ significantly in the class compared to the whole samples. Only the  
385 most remarkable test values have been reported with their significance level ( $*p < 0.05$ ;  $**p$   
386  $< 0.01$ ;  $***p < 0.001$ ). Values in italic are close to -2 and +2 corresponding to  $p < 0.05$ .

387

388  
389  
390  
391

Category		Class 1	Class 2	Class 3
<b>Fraction</b>	<b>WSE</b>	2.50*		-2,15*
	<b>PM</b>	-2.18*		1,51 ( <i>p</i> =0,13)
<b>Influence</b>	<b>I</b>	3.05**	-2.02*	
	<b>U-A</b>		-1.75 ( <i>p</i> =0.08)	2,05*
	<b>U-Su</b>	-2.02*	2.92**	
	<b>U-Y</b>		1.59 ( <i>p</i> =0.11)	
<b>cellular parameter</b>	<b>ROS</b>	-6.04***	2.93**	4,11***
	<b>carbonylated proteins</b>	-4.70***		4,82***
	<b>8-isoprostane</b>	-4.34***	2.62**	2,20*
	<b>8-OHdG</b>	-1.89 ( <i>p</i> =0.06)	-2.08*	5,71***
	<b>IL-6</b>	-1.66 ( <i>p</i> =0.10)		

392

393

#### 394 4. Discussion

395 Regardless the site typology and the season, cell exposure to particles as a whole (PM) and  
396 dPM caused a significant increase (*p* <0.001; Figure S2) in the secretion of the pro-  
397 inflammatory cytokine interleukin-6. To a lesser extent, organic extracts gave the same effect,  
398 whereas exposure to water-soluble extracts showed no effect. Several studies have already  
399 reported the greater ability of particulate samples to induce an inflammatory response compared  
400 to their water-soluble (Shang et al., 2020) or organic extracts (Badran et al., 2020b; Verdin et  
401 al., 2017). As observed in this work, the literature also reported no inflammatory response  
402 following exposure of BEAS-2B cells to water-soluble and/or organic extracts (Chowdhury et  
403 al., 2018; Honda et al., 2017). A recent study showed that particles deprived of their organic or  
404 water-soluble fractions were able to induce inflammation (TNF- $\alpha$ ) to a greater degree than  
405 organic and water-soluble fractions (Gali et al., 2019). Our observations are in line with these  
406 previous findings, pointing out the important contribution of the particulate skeleton in

407 triggering the inflammatory response. The latter has been widely described in the literature as  
408 intimately linked to the initiation of cellular oxidative stress, including a strong link between  
409 the secretion of pro-inflammatory interleukins and the accumulation of ROS (Dergham et al.,  
410 2015; Jiang et al., 2020; Symon et al., 2020; Xu et al., 2018).

411

412 In this study, attention was also paid on the possible development of a cellular oxidative stress.  
413 It appeared that BEAS-2B cells exposed to the different PM<sub>2.5-0.3</sub> samples/fractions exhibited  
414 ROS accumulation under all exposure conditions, whatever the fraction considered (PM, OE,  
415 WSE, dPM). In the literature, several studies had already demonstrated the ability of airborne  
416 particulate extracts to generate ROS accumulation in cells, either after exposure to their organic  
417 (Libalova et al., 2018; Rodríguez-Cotto et al., 2015; Yan et al., 2017) or water-soluble fractions  
418 (Q. Liu et al., 2020; Shuster-Meiseles et al., 2016; Xu et al., 2018; Yan et al., 2017). Several  
419 recent studies have highlighted the significant contribution of metals in ROS generation,  
420 especially the elements As, Bi, Ce, Cd, Cr, Co, Cu, Mo, Ni, Pb, Sb, Se, Sn, V and Zn (Crobeddu  
421 et al., 2020; Das et al., 2021; Fang et al., 2020). The relatively high contents of PAHs, water  
422 soluble ions and elements (Cr, Co, Cu, Sn, NO<sub>3</sub><sup>-</sup>, Al, Cu, Pb, Sn and V) in the "Traffic" and the  
423 different "Urban" samples could also explain their strong capacity to generate ROS in cells.  
424 This is also the case for the sample collected under industrial influence (I), particularly rich in  
425 PAH (136 µg/g) and in Co, Cr, Mn, Ni and V (Table 1). It is to note that a preponderant effect  
426 in ROS accumulation was shown for the particulate fraction comparing to the moderate effect  
427 obtained with water-soluble and organic extracts.

428

429 Concerning the cell membrane damages assessed by the 8-isoprostane quantification, only a  
430 trend could be revealed for PM<sub>2.5-0.3</sub> samples. However, recent studies have demonstrated the  
431 ability of airborne particles to alter the cell membrane. Badran et al, (2020) showed that

432 particulate samples induced a more pronounced membrane alteration than their organic  
433 extracts, which also appeared to be the trend here, although the difference was not significant.

434

435 Focusing on the DNA damages, 8-OHdG did not show significant difference between most of  
436 the different PM<sub>2.5-0.3</sub> fractions. However, the effect of PM and OE fractions seemed to be  
437 predominant. This result is confirmed by several statistical analyses, in particular the PCA and  
438 classification (Figure 3; Figure S3), which showed a clear discrimination between the effect of  
439 the particulate fractions and the organic and then water-soluble extracts. Results are in  
440 agreement with works that have demonstrated the ability of the particles themselves (Dergham  
441 et al., 2015, 2012; Leclercq et al., 2018) or their organic extracts (Abbas et al., 2019; Badran et  
442 al., 2020b; Billet et al., 2018) to induce oxidative DNA damages, by 8-OHdG determination.  
443 Similarly, other authors have also highlighted the genotoxic effects triggered by atmospheric  
444 fine particles, notably by the phospho-H2AX assay (Borgie et al., 2015), and the assessment of  
445 DNA damage via the comet (Gualtieri et al., 2011; Platel et al., 2020).

446

447 Concerning carbonylated proteins, our observations are in agreement with Ndong Ba et al,  
448 (2019) who demonstrated, the ability of atmospheric particles to trigger cellular protein  
449 oxidation on the BEAS-2B cell line. Recently, Badran et al, (2020) also found that PM could  
450 induce more oxidative damage to proteins than their organic extracts did.

451

452 The correlation analysis has revealed a weak positive correlation ( $r=0.33$ ,  $p < 0.01$ ) between  
453 cellular ROS concentration and IL-6 secretion. This hyper accumulation of ROS in the cell is  
454 often described as being associated with alterations in biological macromolecules (Cachon et  
455 al., 2014; Cui et al., 2020; Dergham et al., 2012; Dieme et al., 2012; Van Den Heuvel et al.,  
456 2016; Yan et al., 2017). In our work, positive correlations between intracellular ROS

457 accumulation and cell membrane alterations ( $r=0.26$ ,  $p < 0.0128$ ), protein oxidation ( $r=0.67$ ,  $p$   
458  $< 0.001$ ) and oxidative DNA adduct formation ( $r=0.28$ ,  $p < 0.006$ ) were found. Indeed, the  
459 predominant impact of the particulate fraction (as a whole or free of organic and water-soluble  
460 fractions) compared to the other fractions was observed on the irreversible oxidation of proteins  
461 by the determination of carbonylated proteins ( $p < 0.01$ ).

462  
463 In this study, positive correlations were found between several elements and oxidative stress  
464 biomarkers. Numerous elements such as Al, As, Cd, Cr, Co, Cu, Pb, Sr, V, Zn, etc are known  
465 to play a major role in ROS generation and oxidative damages (Crobeddu et al., 2017; Das et  
466 al., 2021; Shuster-Meiseles et al., 2016). Indeed, Al and Pb have already been described to be  
467 associated with redox reactions (Verstraeten et al., 2008) while Cr, As and Cd, carcinogenic to  
468 human elements (IARC, 2012) can induce the overproduction of ROS in cells and thus  
469 contribute to plasma membrane alterations as well as to protein and DNA damages (Chen and  
470 Lippmann, 2009; Fortoul et al., 2015). Exposure of BEAS-2B cells to  $TiO_2$  has been shown to  
471 induce ROS generation, increased 8-OHdG concentrations, lipid peroxidation (Bhattacharya et  
472 al., 2009; Gurr et al., 2005). ZnO has been previously described to induce ROS overproduction,  
473 protein oxidation, DNA damages, lipid peroxidation (Huang et al., 2010; Saliani et al., 2016;  
474 Singh et al., 2020; Syama et al., 2013; Zoufan et al., 2020).

475  
476 In this work, correlations were found between the contents of some light PAHs in  $PM_{2.5-0.3}$  and  
477 oxidative damage to proteins (acy:  $r=0.33$ ,  $p < 0.05$ ; ace:  $r=0.42$ ,  $p < 0.01$ ), cell membranes  
478 (ace:  $r=0.56$ ,  $p < 0.001$ ; phe:  $r=0.42$ ,  $p < 0.001$ ; ant:  $r=0.37$ ,  $p < 0.01$ ; fla:  $r=0.36$ ,  $p < 0.05$ ;  
479 pyr:  $r=0.35$ ,  $p < 0.05$ ) as well as to DNA (nap:  $r=0.37$ ,  $p < 0.05$ ; ace:  $r=0.46$ ,  $p < 0.01$ ). It has  
480 already been shown in the literature that these PAHs are capable of inducing ROS  
481 overproduction, lipid peroxidation and DNA damage (Ma et al., 2019; Machado et al., 2014;

482 Vuchetich et al., 1996; Wang and Zheng, 2008). In addition, PAHs in PM<sub>2.5</sub> have previously  
483 been associated with the induction of oxidative stress and inflammation in human bronchial cell  
484 models (Boublil et al., 2013; Dergham et al., 2015, 2012; Leclercq et al., 2018). Similarly, the  
485 particulate and organic fractions of the traffic-influenced sample (T) and the urban samples  
486 collected during cold seasons (U-A and U-W) were found to be among the most toxic across  
487 all tests performed. For the urban samples, the total PAH content of these samples (79 and 85  
488 µg/g for U-A and U-W respectively) and trace elements such as Al, As, Cd, Cr, Co, Cu, Pb, Sr,  
489 and Zn could be involved in the level of cell response. Indeed, PAH contents were 3 to 4 times  
490 higher in particles collected during cold seasons compared to warm seasons (U-W=85; U-  
491 A=79; U-Sp=25 and U-Su=21 µg/g PM).

492  
493 On the basis of the contents of organic and inorganic compounds, it appeared surprising that  
494 the sample collected under industrial influence (I), whether for its particulate fraction or its  
495 water-soluble and organic extracts, was found to show a cell response positioned among the  
496 least toxic samples. This is the case for all the parameters of oxidative stress evaluated (also  
497 highlighted through the PCA/classification). Indeed, this I-PM sample exhibits the highest  
498 contents in PAHs (136 µg/g) (Table 1; Figure S1) and in some trace elements as Cd, Cr, Co,  
499 Pb, Sr and Zn (Table 1), known for exerting toxic effects (Guo et al., 2022; Liu et al., 2022).  
500 However, the same observation had already been made by Dergham et al, (2012), who had also  
501 collected a sample under industrial influence at the same site. Although significantly higher in  
502 organic compounds and metallic elements, the PM<sub>2.5-0.3</sub> sample collected under the same  
503 conditions was found to induce a lower cell response than traffic and urban influence to  
504 oxidative stress parameters. This finding could be explained by the richness of these industrial  
505 samples in Fe (more than twice as concentrated as the other samples) and in particular by the  
506 presence of the Fe<sub>3</sub>O<sub>4</sub> form in the collected PM (Heliot, 2018; Kfoury et al., 2016; Laversin,

507 2006) which is related due to emissions from the nearby steel complex (Hleis et al., 2013).  
508 Indeed, it was shown that the  $\text{Fe}_3\text{O}_4$  form was found in particles emitted at the blast furnace and  
509 steel mill. Complementary tests on BEAS-2B cells were carried out by considering reference  
510 samples, and results showed that  $\text{Fe}_3\text{O}_4$  sample, when considered pure or in mixture with other  
511 metal oxide compounds as  $\text{Mn}_2\text{O}_3$ ,  $\text{ZnO}$  and  $\text{Fe}_2\text{O}_3$ , induced oxidative damages in a lesser extent  
512 than other metal oxides tested.  $\text{Fe}_3\text{O}_4$  is a compound formed at high temperature during in the  
513 industrial process. It associates  $\text{Fe(II)}$  and  $\text{Fe(III)}$  and is less oxidized than  $\text{Fe(III)}$  oxide. This  
514 observation tends to show that  $\text{Fe}_3\text{O}_4$  would exert an inhibiting effect regarding oxidative stress.  
515 A recent study conducted on A549 cells showed that following exposure to the Mn/Pb mixture,  
516 cell viability was 45%, and was higher in the case of the Fe/Mn/Pb mixture (69%), which would  
517 mean that the presence of iron would inhibit the cytotoxicity (Yuan et al., 2019). We also  
518 showed that the  $\text{PM}_{2.5-0.3}$  sample collected under industrial influence (I-PM) have a high  
519 manganese content (6 692  $\mu\text{g/g}$ ) almost 4 times higher than that of the urban sample (Table 1).  
520 However, it was shown through tests performed on the synthetic samples that  $\text{Mn}_2\text{O}_3$  could  
521 cause high ROS production and significant increases in other oxidative stress parameters.  
522 Studies have proven the role of  $\text{Mn}_2\text{O}_3$  in inducing oxidative stress through protein oxidation  
523 and lipid peroxidation (Ognik et al., 2019; Sun et al., 2013). Another recent study showed that  
524 exposure of A549 cells to 79  $\mu\text{g/L}$   $\text{Mn}^{2+}$  could decrease their cell viability (Yuan et al., 2019).  
525 In our case, and considering the oxidative stress results for the industrial sample (I-PM), it can  
526 be suggested that the effect of manganese is limited due to the presence of  $\text{Fe}_3\text{O}_4$  in the PM  
527 sample.

528  
529 Interactions between organic compounds, such as PAHs or even HULIS-type organic  
530 compounds (although not analyzed in our work) with metallic elements cannot be excluded. It  
531 can be suggested that synergistic interactions between metals and organic compounds

532 contribute to the oxidative power of organic compounds such as quinones, which oxidize  
533 cellular antioxidants and subsequently generate H<sub>2</sub>O<sub>2</sub>. The latter can then be converted to OH  
534 radical by metal species, through the Fenton reaction (Wang et al., 2018). This result is in  
535 agreement with those obtained in other recent studies (Al Hanai et al., 2019; Xu et al., 2020).  
536 This type of interaction between PM compounds could also be considered to explain the higher  
537 level of oxidative stress for PM<sub>2.5-0.3</sub> samples at the urban site in the cold season (U-A-PM and  
538 U-W-PM), which are richer in PAHs than the samples collected in spring and summer (U-Sp-  
539 PM and U-Su-PM).  
540 Finally, the four PM fractions and the three studied influences were able to induce oxidative  
541 stress damages, with different levels of magnitude and different target (membrane DNA,  
542 proteins). Oxidative stress is considered as the first mechanism involved in the PM toxicity on  
543 cells and consequently each PM fraction can be an inducer of the whole PM toxicity.

544

## 545 **5. Conclusion**

546 The main objective of this study was to discriminate the effect of different PM<sub>2.5-0.3</sub> fractions  
547 from various origins on the induction of oxidative stress and related damages after exposure of  
548 BEAS-2B cells. The results showed that all fractions tested induced oxidative stress. The PM<sub>2.5-  
549 0.3</sub> particles were able to trigger the overproduction of ROS and cause protein damage at higher  
550 levels than the other fractions. The predominant effect of the particulate fraction on these  
551 parameters (ROS and carbonylated proteins) is confirmed by the results obtained on the dPM  
552 sample, whose response was higher than that measured with the organic and water-soluble  
553 extracts. Correlation analysis showed that ROS concentrations were correlated with  
554 inflammation (IL-6; r=0.33) and with the three oxidative stress-related injury parameters: weak  
555 correlations with 8-OHdG (r=0.28) and 8-isoprostane (r=0.26) concentrations, but strong  
556 correlations with carbonylated protein concentration (r=0.67). On the other hand, oxidative

557 stress parameters showed weak or moderate correlations with some chemical compounds,  
558 whether major and trace metal elements or PAHs. This tends to illustrate the complexity of  
559 interactions between PM constituents, and potentially the existence of additive, synergistic and  
560 antagonistic effects, which may explain the observed results. Principal component analysis  
561 (PCA) showed a correlation between the amount of ROS detected and the 8-isoprostane and  
562 carbonylated protein parameters, whereas 8-OHdG appeared to be completely uncorrelated  
563 with the other oxidative stress damage parameters. Sample collected under industrial influence  
564 appears to be the less linked to cell damages and ROS production in comparison with the other  
565 influences. The classification results confirmed the ability of the particulate fractions to induce  
566 the most damage at the protein and cell membrane level.

567 In order to better understand the synergistic and antagonistic effects between metals and/or  
568 organic compounds, it would be interesting to repeat the same experiments on synthetic  
569 samples, by preparing combinations of metals, carbon black, and by including individual  
570 organic compounds in these mixtures, especially quinones. To go further, it could be relevant  
571 to also study the effect of dose, by preparing synthetic samples with different mass proportions  
572 of the compounds.

573

#### 574 **Acknowledgments**

575 The "Unité de Chimie Environnementale et Interactions sur le Vivant", UCEIV UR4492,  
576 participates in the CLIMIBIO project, which is financially supported by the Hauts-de-France  
577 Region Council, the Ministry of Higher Education and Research, the European Regional  
578 Development Funds. Lamia Moufarrej is grateful to the "Pôle Métropolitain Côte d'Opale"  
579 (PMCO) for the funding of her PhD. PM<sub>2.5-0.3</sub> from the urban site, and from the industrial and  
580 traffic sites were collected and characterized within the framework of the National Research  
581 Program for Environmental and Occupational Health: Projects "Biomarkers of toxicity of

582 particulate air pollution influenced by age, PACATOX" (ANSES, 2014) and "Impact of PM<sub>2.5</sub>  
583 varying according to their source (Road traffic - Industries) on respiratory health. In vitro  
584 approach (TRIPLER)" (ANSES, 2016).

585

586

587

## 588 **References**

- 589 Abbas, I., Badran, G., Verdin, A., Ledoux, F., Roumie, M., Lo Guidice, J.-M., Courcot, D.,  
590 Garçon, G., 2019. In vitro evaluation of organic extractable matter from ambient PM<sub>2.5</sub>  
591 using human bronchial epithelial BEAS-2B cells: Cytotoxicity, oxidative stress, pro-  
592 inflammatory response, genotoxicity, and cell cycle deregulation. *Environ. Res.* 171,  
593 510–522. <https://doi.org/10.1016/j.envres.2019.01.052>
- 594 Al Hanai, A.H., Antkiewicz, D.S., Hemming, J.D.C., Shafer, M.M., Lai, A.M., Arhami, M.,  
595 Hosseini, V., Schauer, J.J., 2019. Seasonal variations in the oxidative stress and  
596 inflammatory potential of PM<sub>2.5</sub> in Tehran using an alveolar macrophage model; The  
597 role of chemical composition and sources. *Environ. Int.* 123, 417–427.  
598 <https://doi.org/10.1016/j.envint.2018.12.023>
- 599 ANSES, 2016. Environnement-Santé-Travail: "Impact des PM<sub>2.5</sub> variant selon leur source  
600 (Trafic routier - Industries) sur la santé respiratoire. Approche in vitro (TRIPLER)."
- 601 ANSES, 2014. Environnement-Santé-Travail: «Biomarqueurs de toxicité de la pollution  
602 atmosphérique particulaire influencés par l'âge, PACATOX »(2015-2017).
- 603 Aryal, A., Harmon, A.C., Dugas, T.R., 2021. Particulate matter air pollutants and  
604 cardiovascular disease: Strategies for intervention. *Pharmacol. Ther.* 223, 107890.  
605 <https://doi.org/10.1016/j.pharmthera.2021.107890>
- 606 Badran, G., Ledoux, F., Verdin, A., Abbas, I., Roumie, M., Genevray, P., Landkocz, Y., Lo  
607 Guidice, J.-M., Garçon, G., Courcot, D., 2020a. Toxicity of fine and quasi-ultrafine  
608 particles: Focus on the effects of organic extractable and non-extractable matter  
609 fractions. *Chemosphere* 243, 125440.  
610 <https://doi.org/10.1016/j.chemosphere.2019.125440>
- 611 Badran, G., Verdin, A., Grare, C., Abbas, I., Achour, D., Ledoux, F., Roumie, M., Cazier, F.,  
612 Courcot, D., Lo Guidice, J.-M., Garçon, G., 2020b. Toxicological appraisal of the  
613 chemical fractions of ambient fine (PM<sub>2.5-0.3</sub>) and quasi-ultrafine (PM<sub>0.3</sub>) particles in  
614 human bronchial epithelial BEAS-2B cells. *Environ. Pollut.* 263, 114620.  
615 <https://doi.org/10.1016/j.envpol.2020.114620>
- 616 Bhattacharya, K., Davoren, M., Boertz, J., Schins, R.P., Hoffmann, E., Dopp, E., 2009.  
617 Titanium dioxide nanoparticles induce oxidative stress and DNA-adduct formation but  
618 not DNA-breakage in human lung cells. *Part. Fibre Toxicol.* 6, 17.  
619 <https://doi.org/10.1186/1743-8977-6-17>
- 620 Billet, S., Landkocz, Y., Martin, P.J., Verdin, A., Ledoux, F., Lepers, C., André, V., Cazier, F.,  
621 Sichel, F., Shirali, P., Gosset, P., Courcot, D., 2018. Chemical characterization of fine  
622 and ultrafine PM, direct and indirect genotoxicity of PM and their organic extracts on

623 pulmonary cells. *J. Environ. Sci. China* 71, 168–178.  
624 <https://doi.org/10.1016/j.jes.2018.04.022>

625 Borgie, M., Ledoux, F., Verdin, A., Cazier, F., Greige, H., Shirali, P., Courcot, D., Dagher, Z.,  
626 2015. Genotoxic and epigenotoxic effects of fine particulate matter from rural and urban  
627 sites in Lebanon on human bronchial epithelial cells. *Environ. Res.* 136, 352–362.  
628 <https://doi.org/10.1016/j.envres.2014.10.010>

629 Boubilil, L., Assémat, E., Borot, M.-C., Boland, S., Martinon, L., Sciare, J., Baeza-Squiban, A.,  
630 2013. Development of a repeated exposure protocol of human bronchial epithelium in  
631 vitro to study the long-term effects of atmospheric particles. *Toxicol. In Vitro* 27, 533–  
632 542. <https://doi.org/10.1016/j.tiv.2012.11.008>

633 Broome, R.A., Powell, J., Cope, M.E., Morgan, G.G., 2020. The mortality effect of PM<sub>2.5</sub>  
634 sources in the Greater Metropolitan Region of Sydney, Australia. *Environ. Int.* 137,  
635 105429. <https://doi.org/10.1016/j.envint.2019.105429>

636 Buoli, M., Grassi, S., Caldiroli, A., Carnevali, G.S., Mucci, F., Iodice, S., Cantone, L., Pergoli,  
637 L., Bollati, V., 2018. Is there a link between air pollution and mental disorders? *Environ.*  
638 *Int.* 118, 154–168. <https://doi.org/10.1016/j.envint.2018.05.044>

639 Cachon, B.F., Firmin, S., Verdin, A., Ayi-Fanou, L., Billet, S., Cazier, F., Martin, P.J., Aissi,  
640 F., Courcot, D., Sanni, A., Shirali, P., 2014. Proinflammatory effects and oxidative  
641 stress within human bronchial epithelial cells exposed to atmospheric particulate matter  
642 (PM<sub>(2.5)</sub> and PM<sub>(>2.5)</sub>) collected from Cotonou, Benin. *Environ. Pollut. Barking Essex*  
643 1987 185, 340–351. <https://doi.org/10.1016/j.envpol.2013.10.026>

644 Chen, C., Liu, C., Chen, R., Wang, W., Li, W., Kan, H., Fu, C., 2018. Ambient air pollution  
645 and daily hospital admissions for mental disorders in Shanghai, China. *Sci. Total*  
646 *Environ.* 613–614, 324–330. <https://doi.org/10.1016/j.scitotenv.2017.09.098>

647 Chen, L.C., Lippmann, M., 2009. Effects of metals within ambient air particulate matter (PM)  
648 on human health. *Inhal. Toxicol.* 21, 1–31.  
649 <https://doi.org/10.1080/08958370802105405>

650 Chowdhury, P.H., Okano, H., Honda, A., Kudou, H., Kitamura, G., Ito, S., Ueda, K., Takano,  
651 H., 2018. Aqueous and organic extract of PM<sub>2.5</sub> collected in different seasons and cities  
652 of Japan differently affect respiratory and immune systems. *Environ. Pollut. Barking*  
653 *Essex* 1987 235, 223–234. <https://doi.org/10.1016/j.envpol.2017.12.040>

654 Crenn, V., Fronval, I., Petitprez, D., Riffault, V., 2017. Fine particles sampled at an urban  
655 background site and an industrialized coastal site in Northern France — Part 1: Seasonal  
656 variations and chemical characterization. *Sci. Total Environ.* 578, 203–218.  
657 <https://doi.org/10.1016/j.scitotenv.2015.11.165>

658 Crobeddu, B., Aragao-Santiago, L., Bui, L.-C., Boland, S., Baeza Squiban, A., 2017. Oxidative  
659 potential of particulate matter <sub>2.5</sub> as predictive indicator of cellular stress. *Environ.*  
660 *Pollut.* 230, 125–133. <https://doi.org/10.1016/j.envpol.2017.06.051>

661 Crobeddu, B., Baudrimont, I., Deweirdt, J., Sciare, J., Badel, A., Camproux, A.-C., Bui, L.C.,  
662 Baeza-Squiban, A., 2020. Lung Antioxidant Depletion: A Predictive Indicator of  
663 Cellular Stress Induced by Ambient Fine Particles. *Environ. Sci. Technol.* 54, 2360–  
664 2369. <https://doi.org/10.1021/acs.est.9b05990>

665 Cui, Y., Chen, G., Yang, Z., 2020. Mitochondrial superoxide mediates PM<sub>2.5</sub>-induced  
666 cytotoxicity in human pulmonary lymphatic endothelial cells. *Environ. Pollut.* 263,  
667 114423. <https://doi.org/10.1016/j.envpol.2020.114423>

668 Das, A., Habib, G., Vivekanandan, P., Kumar, A., 2021. Reactive oxygen species production  
669 and inflammatory effects of ambient PM<sub>2.5</sub>-associated metals on human lung epithelial  
670 A549 cells “one year-long study”: The Delhi chapter. *Chemosphere* 262, 128305.  
671 <https://doi.org/10.1016/j.chemosphere.2020.128305>

- 672 Dergham, M., Lepers, C., Verdin, A., Billet, S., Cazier, F., Courcot, D., Shirali, P., Garçon, G.,  
673 2012. Prooxidant and proinflammatory potency of air pollution particulate matter  
674 (PM<sub>2.5-0.3</sub>) produced in rural, urban, or industrial surroundings in human bronchial  
675 epithelial cells (BEAS-2B). *Chem. Res. Toxicol.* 25, 904–919.  
676 <https://doi.org/10.1021/tx200529v>
- 677 Dergham, M., Lepers, C., Verdin, A., Cazier, F., Billet, S., Courcot, D., Shirali, P., Garçon, G.,  
678 2015. Temporal–spatial variations of the physicochemical characteristics of air  
679 pollution Particulate Matter (PM<sub>2.5-0.3</sub>) and toxicological effects in human bronchial  
680 epithelial cells (BEAS-2B). *Environ. Res.* 137, 256–267.  
681 <https://doi.org/10.1016/j.envres.2014.12.015>
- 682 Dieme, D., Cabral-Ndior, M., Garçon, G., Verdin, A., Billet, S., Cazier, F., Courcot, D., Diouf,  
683 A., Shirali, P., 2012. Relationship between physicochemical characterization and  
684 toxicity of fine particulate matter (PM<sub>2.5</sub>) collected in Dakar city (Senegal). *Environ.*  
685 *Res.* 113, 1–13. <https://doi.org/10.1016/j.envres.2011.11.009>
- 686 Dong, Y., Liao, L., Li, L., Yi, F., Meng, H., He, Y., Guo, M., 2019. Skin inflammation induced  
687 by ambient particulate matter in China. *Sci. Total Environ.* 682, 364–373.  
688 <https://doi.org/10.1016/j.scitotenv.2019.05.155>
- 689 Fang, Y., Xing, C., Wang, X., Cao, H., Zhang, C., Guo, X., Zhuang, Y., Hu, R., Hu, G., Yang,  
690 F., 2020. Activation of the ROS/HO-1/NQO1 signaling pathway contributes to the Cu-  
691 induced oxidative stress and autophagy in duck renal tubular epithelial cells. *Sci. Total*  
692 *Environ.* 143753. <https://doi.org/10.1016/j.scitotenv.2020.143753>
- 693 Favez, O., Petit, J.-E., Bessagnet, B., Meleux, F., Chiappini, L., Lemeur, S., Labartette, C.,  
694 Chappaz, C., Guernion, P.-Y., Saison, J.-Y., Chretien, E., Pallares, C., Verlhac, S.,  
695 Aujay, R., Malherbe, L., Beauchamp, M., Piot, C., Jaffrezo, J.-L., Besombes, J.-L.,  
696 Sciare, J., Rouil, L., Leoz-Garziandia, E., 2012. Caractéristiques et origines principales  
697 des épisodes de pollution hivernaux aux PM<sub>2.5</sub> en France. *Pollut. Atmos. Clim. Santé*  
698 *Société* 163–181.
- 699 Fischer, P.H., Marra, M., Ameling, C.B., Velders, G.J.M., Hoogerbrugge, R., de Vries, W.,  
700 Wesseling, J., Janssen, N.A.H., Houthuijs, D., 2020. Particulate air pollution from  
701 different sources and mortality in 7.5 million adults — The Dutch Environmental  
702 Longitudinal Study (DUELS). *Sci. Total Environ.* 705, 135778.  
703 <https://doi.org/10.1016/j.scitotenv.2019.135778>
- 704 Fortoul, T.I., Rodriguez-Lara, V., Gonzalez-Villalva, A., Rojas-Lemus, M., Colin-Barenque,  
705 L., Bizarro-Nevarés, P., García-Peláez, I., Ustarroz-Cano, M., López-Zepeda, S.,  
706 Cervantes-Yépez, S., López-Valdez, N., Meléndez-García, N., Espinosa-Zurutuza, M.,  
707 Cano-Rodríguez, G.C.-G. and M.C., 2015. Health Effects of Metals in Particulate  
708 Matter. *Curr. Air Qual. Issues* 654. <https://doi.org/10.5772/59749>
- 709 Gali, N.K., Li, G., Ning, Z., Brimblecombe, P., 2019. Diurnal trends in redox characteristics of  
710 water-soluble and -insoluble PM components. *Environ. Pollut.* 254, 112841.  
711 <https://doi.org/10.1016/j.envpol.2019.07.009>
- 712 Gogna, P., Narain, T.A., O’Sullivan, D.E., Villeneuve, P.J., Demers, P.A., Hystad, P., Brenner,  
713 D.R., Friedenreich, C.M., King, W.D., 2019. Estimates of the current and future burden  
714 of lung cancer attributable to PM<sub>2.5</sub> in Canada. *Prev. Med., Burden of Cancer in Canada*  
715 122, 91–99. <https://doi.org/10.1016/j.ypmed.2019.03.010>
- 716 Gualtieri, M., Ovrevik, J., Mollerup, S., Asare, N., Longhin, E., Dahlman, H.-J., Camatini, M.,  
717 Holme, J.A., 2011. Airborne urban particles (Milan winter-PM<sub>2.5</sub>) cause mitotic arrest  
718 and cell death: Effects on DNA, mitochondria, AhR binding and spindle organization.  
719 *Mutat. Res.* 713, 18–31. <https://doi.org/10.1016/j.mrfmmm.2011.05.011>

- 720 Guan, Y., Xiao, Y., Wang, F., Qiu, X., Zhang, N., 2021. Health impacts attributable to ambient  
721 PM<sub>2.5</sub> and ozone pollution in major Chinese cities at seasonal-level. *J. Clean. Prod.*  
722 311, 127510. <https://doi.org/10.1016/j.jclepro.2021.127510>
- 723 Guo, L.-C., Lv, Z., Ma, W., Xiao, J., Lin, H., He, G., Li, X., Zeng, W., Hu, J., Zhou, Y., Li, M.,  
724 Yu, S., Xu, Y., Zhang, J., Zhang, H., Liu, T., 2022. Contribution of heavy metals in  
725 PM<sub>2.5</sub> to cardiovascular disease mortality risk, a case study in Guangzhou, China.  
726 *Chemosphere* 297, 134102. <https://doi.org/10.1016/j.chemosphere.2022.134102>
- 727 Gurr, J.-R., Wang, A.S.S., Chen, C.-H., Jan, K.-Y., 2005. Ultrafine titanium dioxide particles  
728 in the absence of photoactivation can induce oxidative damage to human bronchial  
729 epithelial cells. *Toxicology* 213, 66–73. <https://doi.org/10.1016/j.tox.2005.05.007>
- 730 Heliot, A., 2018. Étude de la réponse cellulaire et des Vésicules Extracellulaires produites par  
731 des macrophages primaires exposés aux particules fines (PM<sub>2.5</sub>) (Thèse de doctorat).  
732 Université du Littoral-Côte d'Opale, France.
- 733 Hleis, D., Fernández-Olmo, I., Ledoux, F., Kfoury, A., Courcot, L., Desmonts, T., Courcot, D.,  
734 2013. Chemical profile identification of fugitive and confined particle emissions from  
735 an integrated iron and steelmaking plant. *J. Hazard. Mater.* 250–251, 246–255.  
736 <https://doi.org/10.1016/j.jhazmat.2013.01.080>
- 737 Ho, E., Karimi Galougahi, K., Liu, C.-C., Bhindi, R., Figtree, G.A., 2013. Biological markers  
738 of oxidative stress: Applications to cardiovascular research and practice. *Redox Biol.* 1,  
739 483–491. <https://doi.org/10.1016/j.redox.2013.07.006>
- 740 Honda, A., Fukushima, W., Oishi, M., Tsuji, K., Sawahara, T., Hayashi, T., Kudo, H., Kashima,  
741 Y., Takahashi, K., Sasaki, H., Ueda, K., Takano, H., 2017. Effects of Components of  
742 PM<sub>2.5</sub> Collected in Japan on the Respiratory and Immune Systems. *Int. J. Toxicol.* 36,  
743 153–164. <https://doi.org/10.1177/1091581816682224>
- 744 Huang, C.-C., Aronstam, R.S., Chen, D.-R., Huang, Y.-W., 2010. Oxidative stress, calcium  
745 homeostasis, and altered gene expression in human lung epithelial cells exposed to ZnO  
746 nanoparticles. *Toxicol. In Vitro* 24, 45–55. <https://doi.org/10.1016/j.tiv.2009.09.007>
- 747 IARC, 2012. IARC monographs on the evaluation of carcinogenic risks to humans, volume 100  
748 C, arsenic, metals, fibres, and dusts: this publication represents the views and expert  
749 opinions of an IARC Working Group on the Evaluation of Carcinogenic Risks to  
750 Humans. IARC, Lyon.
- 751 Jan, R., Roy, R., Bhor, R., Pai, K., Satsangi, P.G., 2020. Toxicological screening of airborne  
752 particulate matter in atmosphere of Pune: Reactive oxygen species and cellular toxicity.  
753 *Environ. Pollut.* 261, 113724. <https://doi.org/10.1016/j.envpol.2019.113724>
- 754 Jiang, N., Wen, H., Zhou, M., Lei, T., Shen, J., Zhang, D., Wang, R., Wu, H., Jiang, S., Li, W.,  
755 2020. Low-dose combined exposure of carboxylated black carbon and heavy metal lead  
756 induced potentiation of oxidative stress, DNA damage, inflammation, and apoptosis in  
757 BEAS-2B cells. *Ecotoxicol. Environ. Saf.* 206, 111388.  
758 <https://doi.org/10.1016/j.ecoenv.2020.111388>
- 759 Kfoury, A., Ledoux, F., Roche, C., Delmaire, G., Roussel, G., Courcot, D., 2016. PM<sub>2.5</sub> source  
760 apportionment in a French urban coastal site under steelworks emission influences using  
761 constrained non-negative matrix factorization receptor model. *J. Environ. Sci. China* 40,  
762 114–128. <https://doi.org/10.1016/j.jes.2015.10.025>
- 763 Lam, J., Sutton, P., Kalkbrenner, A., Windham, G., Halladay, A., Koustas, E., Lawler, C.,  
764 Davidson, L., Daniels, N., Newschaffer, C., Woodruff, T., 2016. A Systematic Review  
765 and Meta-Analysis of Multiple Airborne Pollutants and Autism Spectrum Disorder.  
766 *PloS One* 11, e0161851. <https://doi.org/10.1371/journal.pone.0161851>
- 767 Landkocz, Y., Ledoux, F., André, V., Cazier, F., Genevray, P., Dewaele, D., Martin, P.J.,  
768 Lepers, C., Verdin, A., Courcot, L., Boushina, S., Sichel, F., Gualtieri, M., Shirali, P.,  
769 Courcot, D., Billet, S., 2017. Fine and ultrafine atmospheric particulate matter at a multi-

770 influenced urban site: Physicochemical characterization, mutagenicity and cytotoxicity.  
771 Environ. Pollut. 221, 130–140. <https://doi.org/10.1016/j.envpol.2016.11.054>

772 Laversin, H., 2006. Traceurs et formes chimiques du fer dans les particules émises dans  
773 l’atmosphère depuis un site sidérurgique : étude spectroscopique et caractérisation de  
774 composés de référence et de particules collectées dans l’environnement (These de  
775 doctorat). Université du Littoral Côte d’Opale.

776 Leclercq, B., Kluza, J., Antherieu, S., Sotty, J., Alleman, L.Y., Perdrix, E., Loyens, A.,  
777 Coddeville, P., Lo Guidice, J.-M., Marchetti, P., Garçon, G., 2018. Air pollution-derived  
778 PM<sub>2.5</sub> impairs mitochondrial function in healthy and chronic obstructive pulmonary  
779 diseased human bronchial epithelial cells. Environ. Pollut. Barking Essex 1987 243,  
780 1434–1449. <https://doi.org/10.1016/j.envpol.2018.09.062>

781 Li, Jianjun, Li, Jin, Wang, G., Ho, K.F., Dai, W., Zhang, T., Wang, Q., Wu, C., Li, Lijuan, Li,  
782 Li, Zhang, Q., 2021. Effects of atmospheric aging processes on in vitro induced  
783 oxidative stress and chemical composition of biomass burning aerosols. J. Hazard.  
784 Mater. 401, 123750. <https://doi.org/10.1016/j.jhazmat.2020.123750>

785 Libalova, H., Milcova, A., Cervena, T., Vrbova, K., Rossnerova, A., Novakova, Z., Topinka,  
786 J., Rossner, P., 2018. Kinetics of ROS generation induced by polycyclic aromatic  
787 hydrocarbons and organic extracts from ambient air particulate matter in model human  
788 lung cell lines. Mutat. Res. Genet. Toxicol. Environ. Mutagen. 827, 50–58.  
789 <https://doi.org/10.1016/j.mrgentox.2018.01.006>

790 Lin, Y.-C., Zhang, Y.-L., Song, W., Yang, X., Fan, M.-Y., 2020. Specific sources of health  
791 risks caused by size-resolved PM-bound metals in a typical coal-burning city of  
792 northern China during the winter haze event. Sci. Total Environ. 734, 138651.  
793 <https://doi.org/10.1016/j.scitotenv.2020.138651>

794 Liu, J., Cao, H., Zhang, Y., Chen, H., 2022. Potential years of life lost due to PM<sub>2.5</sub>-bound  
795 toxic metal exposure: Spatial patterns across 60 cities in China. Sci. Total Environ. 812,  
796 152593. <https://doi.org/10.1016/j.scitotenv.2021.152593>

797 Liu, Q., Lu, Z., Xiong, Y., Huang, F., Zhou, J., Schauer, J.J., 2020. Oxidative potential of  
798 ambient PM<sub>2.5</sub> in Wuhan and its comparisons with eight areas of China. Sci. Total  
799 Environ. 701, 134844. <https://doi.org/10.1016/j.scitotenv.2019.134844>

800 Liu, X., Zhao, X., Li, X., Lv, S., Ma, R., Qi, Y., Abulikemu, A., Duan, H., Guo, C., Li, Y., Sun,  
801 Z., 2020. PM<sub>2.5</sub> triggered apoptosis in lung epithelial cells through the mitochondrial  
802 apoptotic way mediated by a ROS-DRP1-mitochondrial fission axis. J. Hazard. Mater.  
803 397, 122608. <https://doi.org/10.1016/j.jhazmat.2020.122608>

804 Ma, J.-K., Saad Eldin, W.F., El-Ghareeb, W.R., Elhelaly, A.E., Khedr, M.H.E., Li, X., Huang,  
805 X.-C., 2019. Effects of Pyrene on Human Liver HepG2 Cells: Cytotoxicity, Oxidative  
806 Stress, and Transcriptomic Changes in Xenobiotic Metabolizing Enzymes and  
807 Inflammatory Markers with Protection Trial Using Lycopene [WWW Document].  
808 BioMed Res. Int. <https://doi.org/10.1155/2019/7604851>

809 Machado, A.A. de S., Hoff, M.L.M., Klein, R.D., Cordeiro, G.J., Lencina Avila, J.M., Costa,  
810 P.G., Bianchini, A., 2014. Oxidative stress and DNA damage responses to phenanthrene  
811 exposure in the estuarine guppy *Poecilia vivipara*. Mar. Environ. Res. 98, 96–105.  
812 <https://doi.org/10.1016/j.marenvres.2014.03.013>

813 Migdal, C., Serres, M., 2011. Espèces réactives de l’oxygène et stress oxydant.  
814 médecine/sciences 27, 405–412. <https://doi.org/10.1051/medsci/2011274017>

815 Morrow, J.D., Awad, J.A., Boss, H.J., Blair, I.A., Roberts, L.J., 1992. Non-cyclooxygenase-  
816 derived prostanoids (F<sub>2</sub>-isoprostanes) are formed in situ on phospholipids. Proc. Natl.  
817 Acad. Sci. U. S. A. 89, 10721–10725.

- 818 Moufarrej, L., 2021. Etude du potentiel oxydant des PM<sub>2.5</sub> et du stress oxydant induit sur les  
819 cellules épithéliales bronchiques BEAS-2B (These de doctorat). Université du Littoral  
820 Côte d'Opale.
- 821 Mu, G., Zhou, M., Wang, B., Cao, L., Yang, S., Qiu, W., Nie, X., Ye, Z., Zhou, Y., Chen, W.,  
822 2021. Personal PM<sub>2.5</sub> exposure and lung function: Potential mediating role of  
823 systematic inflammation and oxidative damage in urban adults from the general  
824 population. *Sci. Total Environ.* 755, 142522.  
825 <https://doi.org/10.1016/j.scitotenv.2020.142522>
- 826 Nagel, G., Stafoggia, M., Pedersen, M., Andersen, Z.J., Galassi, C., Munkenast, J., Jaensch, A.,  
827 Sommar, J., Forsberg, B., Olsson, D., Oftedal, B., Krog, N.H., Aamodt, G., Pyko, A.,  
828 Pershagen, G., Korek, M., Faire, U.D., Pedersen, N.L., Östenson, C.-G., Fratiglioni, L.,  
829 Sørensen, M., Tjønneland, A., Peeters, P.H., Bueno-de-Mesquita, B., Vermeulen, R.,  
830 Eeftens, M., Plusquin, M., Key, T.J., Concin, H., Lang, A., Wang, M., Tsai, M.-Y.,  
831 Grioni, S., Marcon, A., Krogh, V., Ricceri, F., Sacerdote, C., Ranzani, A., Cesaroni, G.,  
832 Forastiere, F., Tamayo-Uria, I., Amiano, P., Dorronsoro, M., Hoogh, K. de, Beelen, R.,  
833 Vineis, P., Brunekreef, B., Hoek, G., Raaschou-Nielsen, O., Weinmayr, G., 2018. Air  
834 pollution and incidence of cancers of the stomach and the upper aerodigestive tract in  
835 the European Study of Cohorts for Air Pollution Effects (ESCAPE). *Int. J. Cancer* 143,  
836 1632–1643. <https://doi.org/10.1002/ijc.31564>
- 837 Ndong Ba, A., Cazier, F., Verdin, A., Garçon, G., Cabral, M., Courcot, L., Diouf, A., Courcot,  
838 D., Gualtieri, M., Fall, M., 2019. Physico-chemical characterization and in vitro  
839 inflammatory and oxidative potency of atmospheric particles collected in Dakar city's  
840 (Senegal). *Environ. Pollut. Barking Essex* 1987 245, 568–581.  
841 <https://doi.org/10.1016/j.envpol.2018.11.026>
- 842 Ognik, K., Kozłowski, K., Stepiñowska, A., Szlązak, R., Tutaj, K., Zduńczyk, Z., Jankowski,  
843 J., 2019. The effect of manganese nanoparticles on performance, redox reactions and  
844 epigenetic changes in turkey tissues. *Anim. Int. J. Anim. Biosci.* 13, 1137–1144.  
845 <https://doi.org/10.1017/S1751731118002653>
- 846 Oravisjärvi, K., Timonen, K.L., Wiikinkoski, T., Ruuskanen, A.R., Heinänen, K., Ruuskanen,  
847 J., 2003. Source contributions to PM<sub>2.5</sub> particles in the urban air of a town situated close  
848 to a steel works. *Atmos. Environ.* 37, 1013–1022. [https://doi.org/10.1016/S1352-2310\(02\)01048-8](https://doi.org/10.1016/S1352-2310(02)01048-8)
- 850 Oudin, A., Bråbäck, L., Åström, D.O., Strömgren, M., Forsberg, B., 2016. Association between  
851 neighbourhood air pollution concentrations and dispensed medication for psychiatric  
852 disorders in a large longitudinal cohort of Swedish children and adolescents. *BMJ Open*  
853 6, e010004. <https://doi.org/10.1136/bmjopen-2015-010004>
- 854 Platel, A., Privat, K., Talahari, S., Delobel, A., Dourdin, G., Gateau, E., Simar, S., Saleh, Y.,  
855 Sotty, J., Antherieu, S., Canivet, L., Alleman, L.-Y., Perdrix, E., Garçon, G., Denayer,  
856 F.O., Lo Guidice, J.M., Nessler, F., 2020. Study of in vitro and in vivo genotoxic  
857 effects of air pollution fine (PM<sub>2.5-0.18</sub>) and quasi-ultrafine (PM<sub>0.18</sub>) particles on lung  
858 models. *Sci. Total Environ.* 711, 134666.  
859 <https://doi.org/10.1016/j.scitotenv.2019.134666>
- 860 Quezada-Maldonado, E.M., Sánchez-Pérez, Y., Chirino, Y.I., García-Cuellar, C.M., 2021.  
861 Airborne particulate matter induces oxidative damage, DNA adduct formation and  
862 alterations in DNA repair pathways. *Environ. Pollut.* 287, 117313.  
863 <https://doi.org/10.1016/j.envpol.2021.117313>
- 864 Rodríguez-Cotto, R.I., Ortiz-Martínez, M.G., Jiménez-Vélez, B.D., 2015. Organic extracts  
865 from African dust storms stimulate oxidative stress and induce inflammatory responses  
866 in human lung cells through Nrf2 but not NF-κB. *Environ. Toxicol. Pharmacol.* 39, 845–  
867 856. <https://doi.org/10.1016/j.etap.2015.02.015>

- 868 Saliani, M., Jalal, R., Goharshadi, E.K., 2016. Mechanism of oxidative stress involved in the  
869 toxicity of ZnO nanoparticles against eukaryotic cells. *Nanomedicine J.* 3, 1–14.  
870 <https://doi.org/10.7508/nmj.2016.01.001>
- 871 Santacatalina, M., Reche, C., Minguillón, M.C., Escrig, A., Sanfelix, V., Carratalá, A., Nicolás,  
872 J.F., Yubero, E., Crespo, J., Alastuey, A., Monfort, E., Miró, J.V., Querol, X., 2010.  
873 Impact of fugitive emissions in ambient PM levels and composition: A case study in  
874 Southeast Spain. *Sci. Total Environ.* 408, 4999–5009.  
875 <https://doi.org/10.1016/j.scitotenv.2010.07.040>
- 876 Shang, J., Zhang, Y., Schauer, J.J., Tian, J., Hua, J., Han, T., Fang, D., An, J., 2020.  
877 Associations between source-resolved PM<sub>2.5</sub> and airway inflammation at urban and  
878 rural locations in Beijing. *Environ. Int.* 139, 105635.  
879 <https://doi.org/10.1016/j.envint.2020.105635>
- 880 Shuster-Meiseles, T., Heo, J., Pardo, M., Antkiewicz, D., Schauer, J., Rudich, A., Rudich, Y.,  
881 2016. ROS-generating/ARE-activating capacity of metals in roadway particulate matter  
882 deposited in urban environment. *Environ. Res.* 146, 252–262.  
883 <https://doi.org/10.1016/j.envres.2016.01.009>
- 884 Singh, R., Cheng, S., Singh, S., 2020. Oxidative stress-mediated genotoxic effect of zinc oxide  
885 nanoparticles on *Deinococcus radiodurans*. *3 Biotech* 10.  
886 <https://doi.org/10.1007/s13205-020-2054-4>
- 887 Sun, W., Luna-Velasco, A., Sierra-Alvarez, R., Field, J.A., 2013. Assessing protein oxidation  
888 by inorganic nanoparticles with enzyme-linked immunosorbent assay (ELISA).  
889 *Biotechnol. Bioeng.* 110, 694–701. <https://doi.org/10.1002/bit.24754>
- 890 Syama, S., Reshma, S.C., Sreekanth, P.J., Varma, H.K., Mohanan, P.V., 2013. Effect of Zinc  
891 Oxide nanoparticles on cellular oxidative stress and antioxidant defense mechanisms in  
892 mouse liver. *Toxicol. Environ. Chem.* 95, 495–503.  
893 <https://doi.org/10.1080/02772248.2013.789606>
- 894 Symon, T., Gaxiola-Robles, R., Hernández-Camacho, C., Zenteno-Savín, T., 2020. Oxidative  
895 Stress Indicators in Leukocytes from Humans and Bottlenose Dolphins in Response to  
896 a Proinflammatory Challenge. *Free Radic. Biol. Med.*, SfrBM 27th Annual Conference  
897 159, S48. <https://doi.org/10.1016/j.freeradbiomed.2020.10.133>
- 898 Szyszkowicz, M., Willey, J.B., Grafstein, E., Rowe, B.H., Colman, I., 2010. Air pollution and  
899 emergency department visits for suicide attempts in Vancouver, Canada. *Environ.*  
900 *Health Insights* 4, 79–86. <https://doi.org/10.4137/EHL.S5662>
- 901 Telesiński, A., Kiepas-Kokot, A., 2021. Five-Year Enhanced Natural Attenuation of  
902 Historically Coal-Tar-Contaminated Soil: Analysis of Polycyclic Aromatic  
903 Hydrocarbon and Phenol Contents. *Int. J. Environ. Res. Public Health* 18, 2265.  
904 <https://doi.org/10.3390/ijerph18052265>
- 905 Van Den Heuvel, R., Den Hond, E., Govarts, E., Colles, A., Koppen, G., Staelens, J., Mampaey,  
906 M., Janssen, N., Schoeters, G., 2016. Identification of PM<sub>10</sub> characteristics involved in  
907 cellular responses in human bronchial epithelial cells (Beas-2B). *Environ. Res.* 149, 48–  
908 56. <https://doi.org/10.1016/j.envres.2016.04.029>
- 909 Verdin, A., Gobert, J., Genevray, P., Ledoux, F., Billet, S., Cazier, F., Courcot, D., Delattre, F.,  
910 2017. Caractérisation chimique et évaluation des propriétés cytotoxiques, pro-  
911 inflammatoires et génotoxiques de particules fines en suspension dans l'air en milieu  
912 rural. Presented at the 47e congrès du Groupe Français des Pesticides, Nancy, France.
- 913 Verstraeten, S.V., Aimo, L., Oteiza, P.I., 2008. Aluminium and lead: molecular mechanisms of  
914 brain toxicity. *Arch. Toxicol.* 82, 789–802. <https://doi.org/10.1007/s00204-008-0345-3>
- 915 Vuchetich, P.J., Bagchi, D., Bagchi, M., Hassoun, E.A., Tang, L., Stohs, S.J., 1996.  
916 Naphthalene-induced oxidative stress in rats and the protective effects of vitamin E

- 917 succinate. *Free Radic. Biol. Med.* 21, 577–590. <https://doi.org/10.1016/0891->  
918 5849(96)00161-x
- 919 Wang, L., Luo, D., Liu, X., Zhu, J., Wang, F., Li, B., Li, L., 2021. Effects of PM<sub>2.5</sub> exposure  
920 on reproductive system and its mechanisms. *Chemosphere* 264, 128436.  
921 <https://doi.org/10.1016/j.chemosphere.2020.128436>
- 922 Wang, L., Zheng, B., 2008. Toxic effects of fluoranthene and copper on marine diatom  
923 *Phaeodactylum tricornutum*. *J. Environ. Sci.* 20, 1363–1372.  
924 [https://doi.org/10.1016/S1001-0742\(08\)62234-2](https://doi.org/10.1016/S1001-0742(08)62234-2)
- 925 Wang, P., Shen, J., Zhu, S., Gao, M., Ma, J., Liu, J., Gao, J., Zhang, H., 2021. The aggravated  
926 short-term PM<sub>2.5</sub>-related health risk due to atmospheric transport in the Yangtze River  
927 Delta. *Environ. Pollut.* 275, 116672. <https://doi.org/10.1016/j.envpol.2021.116672>
- 928 Wang, Y., Plewa, M.J., Mukherjee, U.K., Verma, V., 2018. Assessing the cytotoxicity of  
929 ambient particulate matter (PM) using Chinese hamster ovary (CHO) cells and its  
930 relationship with the PM chemical composition and oxidative potential. *Atmos.*  
931 *Environ.* 179, 132–141. <https://doi.org/10.1016/j.atmosenv.2018.02.025>
- 932 Xing, W., Yang, L., Zhang, H., Zhang, X., Wang, Y., Bai, P., Zhang, L., Hayakawa, K., Nagao,  
933 S., Tang, N., 2022. Variations in traffic-related polycyclic aromatic hydrocarbons in  
934 PM<sub>2.5</sub> in Kanazawa, Japan, after the implementation of a new vehicle emission  
935 regulation. *J. Environ. Sci.* 121, 38–47. <https://doi.org/10.1016/j.jes.2021.08.046>
- 936 Xu, F., Qiu, X., Hu, X., Shang, Y., Pardo, M., Fang, Y., Wang, J., Rudich, Y., Zhu, T., 2018.  
937 Effects on IL-1 $\beta$  signaling activation induced by water and organic extracts of fine  
938 particulate matter (PM<sub>2.5</sub>) in vitro. *Environ. Pollut. Barking Essex* 1987 237, 592–600.  
939 <https://doi.org/10.1016/j.envpol.2018.02.086>
- 940 Xu, X., Lu, X., Li, X., Liu, Y., Wang, X., Chen, H., Chen, J.-M., Yang, X., Fu, T.-M., Zhao,  
941 Q., Fu, Q., 2020. ROS-generation potential of Humic-like substances (HULIS) in  
942 ambient PM<sub>2.5</sub> in urban Shanghai: Association with HULIS concentration and light  
943 absorbance. *Chemosphere* 256, 127050.  
944 <https://doi.org/10.1016/j.chemosphere.2020.127050>
- 945 Yan, J., Lai, C.-H., Lung, S.-C.C., Chen, C., Wang, W.-C., Huang, P.-I., Lin, C.-H., 2017.  
946 Industrial PM<sub>2.5</sub> cause pulmonary adverse effect through RhoA/ROCK pathway. *Sci.*  
947 *Total Environ.* 599–600, 1658–1666. <https://doi.org/10.1016/j.scitotenv.2017.05.107>
- 948 Yuan, Y., Wu, Y., Ge, X., Nie, D., Wang, M., Zhou, H., Chen, M., 2019. In vitro toxicity  
949 evaluation of heavy metals in urban air particulate matter on human lung epithelial cells.  
950 *Sci. Total Environ.* 678, 301–308. <https://doi.org/10.1016/j.scitotenv.2019.04.431>
- 951 Zhang, Y., Song, Y., Chen, Y.-J., Chen, Y., Lu, Y., Li, R., Dong, C., Hu, D., Cai, Z., 2021.  
952 Discovery of emerging sulfur-containing PAHs in PM<sub>2.5</sub>: Contamination profiles and  
953 potential health risks. *J. Hazard. Mater.* 416, 125795.  
954 <https://doi.org/10.1016/j.jhazmat.2021.125795>
- 955 Zoufan, P., Baroonian, M., Zargar, B., 2020. ZnO nanoparticles-induced oxidative stress in  
956 *Chenopodium murale* L, Zn uptake, and accumulation under hydroponic culture.  
957 *Environ. Sci. Pollut. Res.* 27, 11066–11078. <https://doi.org/10.1007/s11356-020->  
958 07735-2  
959

960

961

962

Accepted Manuscript